Published in final edited form as:

Mol Psychiatry. 2023 October ; 28(10): 4421–4437. doi:10.1038/s41380-023-02216-7.

Transmission of Alzheimer's disease-associated microbiota dysbiosis and its impact on cognitive function: evidence from mice and patients

Yiying Zhang[1,11], **Yuan Shen**[1,2,3,11], **Ning Liufu**[1,4], **Ling Liu**[1,4], **Wei Li**[1], **Zhongyong Shi**[1,2,3], **Hailin Zheng**[2], **Xinchun Mei**[1,2,3], **Chih-Yu Chen**[5], **Zengliang Jiang**[5,6], **Shabnamsadat Abtahi**[7], **Yuanlin Dong**[1], **Feng Liang**[1], **Yujiang Shi**[8], **Leo L. Cheng**[9], **Guang Yang**[10], **Jing X. Kang**[5], **Jeremy E. Wilkinson**[7], **Zhongcong Xie**[1]

[1]Geriatric Anesthesia Research Unit, Department of Anesthesia, Critical Care and Pain Medicine, Massachusetts General Hospital and Harvard Medical School, Charlestown, MA 02129, USA.

[2]Anesthesia and Brain Research Institute, Shanghai Tenth People's Hospital, Tongji University School of Medicine, Shanghai 200072, PR China.

[3]Mental Health Center affiliated to Shanghai Jiao Tong University School of Medicine, Shanghai 200030, PR China.

[4]Department of Anesthesiology, Sun Yat-Sen Memorial Hospital, Sun Yat-Sen University, Guangzhou, Guangdong Province 510120, PR China.

[5]Laboratory for Lipid Medicine and Technology, Department of Medicine, Massachusetts General Hospital and Harvard Medical School, Charlestown, MA 02129, USA.

[6]Key Laboratory of Growth Regulation and Translational Research of Zhejiang Province, School of Life Sciences, Westlake University, Hangzhou, PR China.

[7]Biostatistics Department and Department of Immunology and Infectious Diseases, Harvard School of Public Health, Boston, MA 02115, USA.

[8]Shanghai Key Laboratory of Medical Epigenetics, Institutes of Biomedical Sciences, Zhongshan Hospital, Fudan University, Shanghai 200032, PR China.

[9]Departments of Radiology and Pathology, Massachusetts General Hospital and Harvard Medical School, Charlestown, MA 02129, USA.

Correspondence and requests for materials should be addressed to Yiying Zhang or Zhongcong Xie. yzhang37@mgh.harvard.edu; zxie@mgh.harvard.edu.

AUTHOR CONTRIBUTIONS

Study concept and design: YZ and ZX. Acquisition of data: YZ, YS, NL, LL, WL, ZS, HZ, XM, CYC, SA, and ZJ. Analysis and interpretation of data: YZ, YS, NL, LL, WL, ZS, HZ, XM, CYC, ZJ, SA, and ZJ. Drafting of the manuscript: YZ and ZX. Critical revision of the manuscript for important intellectual content: YZ, YJS, LC, JXK, GY, JK, JW and ZX. Obtained funding: YZ and ZX. Administrative, technical, and material support: YZ, YS, YD, FL and ZX. Study supervision: YZ, YS and ZX.

COMPETING INTERESTS

The authors declare that they have no competing interests. ZX provided consulting services to Shanghai's 9th and 10th hospitals, Baxter (invited speaker), NanoMosaic, and Journal of Anesthesiology and Perioperative Science in the last 36 months.

ADDITIONAL INFORMATION

Supplementary information The online version contains supplementary material available at https://doi.org/10.1038/s41380-023-02216-7.

[10]Department of Anesthesiology, Columbia University Medical Center, New York, NY 10032, USA.

[11]These authors contributed equally: Yiying Zhang, Yuan Shen.

Abstract

Spouses of Alzheimer's disease (AD) patients are at a higher risk of developing incidental dementia. However, the causes and underlying mechanism of this clinical observation remain largely unknown. One possible explanation is linked to microbiota dysbiosis, a condition that has been associated with AD. However, it remains unclear whether gut microbiota dysbiosis can be transmitted from AD individuals to non-AD individuals and contribute to the development of AD pathogenesis and cognitive impairment. We, therefore, set out to perform both animal studies and clinical investigation by co-housing wild-type mice and AD transgenic mice, analyzing microbiota via 16S rRNA gene sequencing, measuring short-chain fatty acid amounts, and employing behavioral test, mass spectrometry, site-mutations and other methods. The present study revealed that co-housing between wild-type mice and AD transgenic mice or administrating feces of AD transgenic mice to wild-type mice resulted in AD-associated gut microbiota dysbiosis, Tau phosphorylation, and cognitive impairment in the wild-type mice. Gavage with Lactobacillus and Bifidobacterium restored these changes in the wild-type mice. The oral and gut microbiota of AD patient partners resembled that of AD patients but differed from healthy controls, indicating the transmission of microbiota. The underlying mechanism of these findings includes that the butyric acid-mediated acetylation of GSK3β at lysine 15 regulated its phosphorylation at serine 9, consequently impacting Tau phosphorylation. Pending confirmative studies, these results provide insight into a potential link between the transmission of AD-associated microbiota dysbiosis and development of cognitive impairment, which underscore the need for further research in this area.

INTRODUCTION

Alzheimer's disease (AD) is the most prevalent dementia among the elderly, with approximately 6.2 million cases in the United States and 24 million worldwide [1]. Despite extensive research, effective treatments and preventative measures for AD have still remain largely to be determined. The pathological hallmarks of AD includes accumulation of beta-amyloid (Aβ) [2], phosphorylation of Tau proteins [3–6, reviewed in 7, 8], and neuroinflammation [9–11]. Nevertheless, our understanding of the regulation of AD pathogenesis and the underlying mechanisms still remains largely unclear.

Gut microbiota (GMB) plays a significant role in brain functions and behavior via microbiota-gut-brain axis [12–14], and gut microbiota dysbiosis have been linked to AD patients and AD pathogenesis [15–18]. Differences in GMB are observed between AD patients and healthy controls [17]. Characteristic alterations in GMB in AD patients include reduced levels of *Eubacterium rectale*, *Firmicutes* and *Bifidobacterium*, and increased levels of *Escherichia/Shigella*, *Bacteroidetes* and *Proteobacteria* compared to healthy control [19–21]. Animal studies have also shown differences in GMB in AD transgenic (Tg) mouse models, including 5XFAD [15, 22], APPSwe/PSEN1dE9 [23–25], and APPSwe/PSEN1L166P [26] strains, compared to wild-type (WT) mice. Brandscheid et al. reported increased *Firmicutes* and decreased *Bacteroidetes phyla* in 5XFAD (5 familial Alzheimer's

disease mutation) mice at 9 weeks compared to WT mice [27]. However, Chen et al. reported the opposite pattern of decreased *Firmicutes* and increased *Bacteroidetes phyla* at 3 months in 5XFAD mice compared to WT mice [15].

Clinical studies have demonstrated that spouses of AD patients have a higher risk of developing incidental dementia [28–33]. Furthermore, stress and emotional well-being can also have a significant impact on the GMB [34]. Both GMB and progression of AD can be regulated by diet [1, 35–38], sleep [39–41] and exercise [42, 43]. These findings suggest that environments factors may contribute to the incidental dementia observed in spouses of AD patients. However, no studies have compared GMB among AD patients, spouses of AD patients and healthy controls. Notably, clinical studies can be challenging due to the required long followup time and confounding factors, making it crucial to understand these potential differences of GMB among AD Tg mice, WT mice co-housed with AD Tg mice and WT mice without co-housing with AD Tg mice. The co-housing of WT mice and AD Tg mice serves as a conceptual model that simulates the cohabitation between individuals with AD and their partners, who also share living spaces and maintain close interactions with AD patients.

Recent studies have shown that the GMB may play a role in regulating β-amyloid (Aβ) accumulation and neuroinflammation in AD and other neurological conditions [44]. Specifically, antibiotics treatment has been shown to alter the GMB composition and Aβ accumulation in AD mouse models [45]. Fecal matter transplants (FMT) from non-antibiotics-treated AD Tg mice to antibiotics-treated AD Tg mice restores the GMB and Aβ accumulation, suggesting a link between GMB changes and Aβ accumulation [46, 47]. Furthermore, antibiotics or germ-free (GF), which can mediate GMB depletion, have been shown to alter microglial inflammatory state [45, 46, 48–50]. Antibiotics also reduce plaque-associated microglia and change microglial morphology [45, 46, 50]. While a few studies have demonstrated the potential transmission of GMB between young AD Tg mice and aged AD Tg mice [15, 16], the transmission of AD pathogenesis and cognitive impairment from AD Tg mice to WT mice through co-housing, along with the underlying mechanisms, remains undetermined.

Considering that GMB may impact AD-associated pathogenesis, it is logical to hypothesize that WT mice co-housed with AD Tg mice obtain AD pathogenesis and develop cognitive impairment through acquiring AD-associated gut microbiota dysbiosis. The present study defined this hypothesis by showing that WT mice co-housed with AD Tg mice for 3 months, referred to as AD-exposed WT (ADWT, the background is still WT mice) mice, acquired AD-related gut microbiota dysbiosis and developed AD pathogenesis and cognitive impairment. The study also revealed that the mechanism underlying this effect that butyric acid, a short-chain fatty acid produced by GMB, mediated-acetylation-regulated phosphorylation in GSK3β, a kinase known to be involved in the phosphorylation of Tau [51, 52]. Additionally, our clinically relevant studies indicated that the partners of AD patients (PAD) acquired GMB profiles similar to AD patients, but different from non-AD controls (CON).

RESULTS

WT mice developed cognitive impairment after co-housing with AD Tg mice

We co-housed two-month-old female WT mice with the same age and gender AD Tg mice for a period up to 3 months, referred to hereafter as the AD-exposed WT (ADWT) mice (Fig. 1a). After the 3 months of co-housing with AD Tg mice, the ADWT mice developed cognitive impairment compared to the WT mice without such co-housing. Specifically, the ADWT mice and AD Tg mice had longer escape latency during the training days (Fig. 1b) and fewer number of platforms crossing on the testing day (Fig. 1c) in Morris water maze (MWM) than the WT mice had. There were no significant differences in swimming speed of MWM among these three groups of mice (Fig. 1d). Similarly, in Barnes maze (BM) test, relative to the WT mice, the ADWT mice and AD Tg mice had longer time to identify and enter the escape box during the training days and on the testing day of BM (Fig. 1e, f), reduced target time (Fig. 1g), more wrong holes searched before entering on the escape box on the testing day of BM (Fig. 1h), and longer distance of BM on the testing day (Fig. 1i). There was no significant difference in speed between the ADWT and WT mice in BM, but the AD Tg mice showed the trend of decreased speed compared to the WT mice (Fig. 1j). The cognitive impairment in ADWT mice was sustained for at least 3 months after the co-housing ended (S-Fig. 1).

Notably, the WT mice co-housed with AD Tg mice only for 1 month did not develop cognitive impairment assessed in MWM and BM (S-Fig. 2), and the AD Tg mice co-housed with WT mice (WTAD, the background is still AD Tg mice) did not show the improved cognitive function compared to the AD Tg mice without such co-housing (S-Fig. 3). These results suggest that the WT mice co-housed with AD Tg mice can develop a time-dependent (1 versus 3 months) and long time (up to 3 months) cognitive impairment.

The study also conducted fecal microbiota transplantation (FMT) experiments to validate that the observed cognitive impairment was due to coprophagia, the re-ingestion of feces, by the ADWT mice. Two-month-old female WT mice were administered with FMT, obtained from 3-month-old female AD Tg (5XFAD) or WT mice, for 7 days (Fig. 2a). Results showed that the WT mice that received fecal microbiota from AD Tg mice developed cognitive impairment evidenced in MWM (Fig. 2b–d) and BM (Fig. 2e–j), while those that received microbiota from WT mice did not (S-Fig. 4).

Further experiments ruled out the confounding influence of airborne transmission and environment on the observed behavior. Specifically, we compared the behavior of mice which had air exchange or in different location. Neither indirect contact via air exchange between AD Tg and WT mice (S-Fig. 5) nor housing of WT mice in a different location for 3 months (S-Fig. 6) caused cognitive impairment in the WT mice. These data suggest that active (co-housing) or passive (FMT) intake of AD Tg mice feces can induce cognitive impairment in the WT mice.

WT mice acquired gut microbiota dysbiosis after co-housing with AD Tg mice

Considering the findings that ADWT mice developed cognitive impairment potentially due to the transfer of GMB from co-housing with AD Tg mice, we then compared the GMB

among AD Tg mice, ADWT mice, and WT mice (Fig. 3a). Principal component analysis (Fig. 3b, S-Fig. 7a, b) demonstrated that the GMB profiling of the ADWT mice (represented by sky blue dots) was similar to that of AD Tg mice (represented by dark blue dots) but different from WT mice (represented by light blue dots). Additionally, the Simpson diversity index (α-diversity) at the operational taxonomic unit (OTU) level showed that Simpson diversity index was significantly higher in AD Tg mice and borderline significant higher in ADWT mice compared to WT mice (Fig. 3c). There were no significant differences in body weight among the three groups of mice (S-Fig. 7c), but the AD Tg and ADWT mice had higher levels of fecal moisture content and weight compared to the WT mice (S-Fig. 7d, e). The heat map in Fig. 3d showed the GMB community profile among the three groups of mice at Genus level.

We then used the Microbiome Multivariable Association with Linear (MaAsLin2) Models [53] to determine the multivariable associations among WT, ADWT, AD Tg mice and their GMB meta-omics features at species levels. Compared to WT mice, the GMB in the ADWT or AD Tg mice was similar and characterized by an increased abundance of proinflammatory bacteria *Dubosiella* [54] and six other bacteria (Fig. 3e–j), but decreased abundances of other bacteria (Fig. 3k–r), which included *Marvinbryantia* (Fig. 3k), the bacteria associated with bowel dysfunction [55]; and anti-inflammatory bacteria *Bacteroides* (Fig. 3l) and *Lactobacillus* [56] (Fig. 3p) compared to WT mice. The abundance of *Faecalibaculum* (Fig. 3m) and *Ruminiclostridium-1*(Fig. 3r), the bacteria associated with short-chain fatty acids (SCFAs) production [57], were also decreased in both AD and ADWT mice compared to those in WT mice.

Notably, AD Tg mice (statistical significance) and ADWT mice (trending) also exhibited increased abundance of *Ruminiclostridium-5* (Fig. 3s), the bacteria associated with mucosa-related microbiome and obesity [58], and decreased abundance of *Lachnoclostridium* (Fig. 3t), a novel marker for colorectal cancer [59], compared to those in WT mice. The quantification of the bacterial taxa association for comparison between WT mice and ADWT mice or AD Tg mice at species levels was presented in S-Table 1. We also demonstrated the correlative relationship of top 15 bacteria at the genus level and found that *Bifidobacterium* and *Lactobacillus* were highly associated in the combined data obtained from AD Tg, ADWT and WT mice (Fig. 3u).

In addition, we observed that AD Tg mice and ADWT mice had decreased amount of butyric acid, one of SCFAs, in their feces compared to WT mice (Fig. 3v). This was consistent with the findings that AD Tg mice and ADWT mice had reduced abundance of *Faecalibaculum* (Fig. 3m) and *Ruminiclostridium-1* (Fig. 3r), the bacteria which generates SCFAs, compared to WT mice.

Finally, there were no significant differences in mucosa, tight junction composition or structure changes in the small intestine or colon between WT mice and AD Tg mice (S-Fig. 8).

ADWT mice exhibited reduced amounts of butyric acid, increased Tau phosphorylation, elevated IL-6 and accumulated Aβ42 and Aβ40 amounts in brain tissues

Building on the previous findings that ADWT mice showed cognitive impairment that might result from the transmitted GMB from AD Tg mice. We further measured the levels of SCFAs in the brain tissues of mice. Our results showed that both AD Tg and ADWT mice exhibited decreases in butyric acid levels in the brain, which was in line with the decrease of butyric acid in feces, compared to WT mice (Fig. 4a). Additionally, we observed changes consistent with AD pathogenesis, including decreased levels of PSD-95, a synaptic marker [60] (Fig. 4b, c), increased levels of Tau phosphorylation, indicated by elevated amounts of Tau-pS202/pT205, Tau-pS262, and Tau-pS199 (Fig. 4b, d, e) in the hippocampus of the AD Tg and ADWT mice, compared to WT mice. The AD Tg and ADWT mice also showed elevated levels of IL-6 (Fig. 4f) and accumulation of Aβ42 and Aβ40 (Fig. 4g) in the hippocampus compared to the WT mice. These findings suggest that the transmission of GMB from AD Tg mice to ADWT mice may play a role in the development of AD pathogenesis, synaptic loss and cognitive impairment in the ADWT mice.

Butyric acid mediated acetylation of GSK3β regulated the phosphorylation GSK3β

Our study found that AD and ADWT mice had higher amounts of Tau-pS202/pT205 in the brain tissues compared to WT mice (Fig. 5a, b), which is associated with AD pathogenesis [61, 62]. We also found that the ratio of phosphorylated (p) GSK3β-S9 to GSK3β was lower in AD and ADWT mice (Fig. 5a, c) compared to WT mice. In vitro experiments showed that butyric acid increased the ratio of p-GSK3β-S9 to GSK3β in HEK 293T cells (Fig. 5d, e). The results of mass spectrometry (MS) studies indicated that the acetylation of GSK3β at lysine 15 (K15) (Fig. 5f). The mutation of lysine (K) 15 to arginine (R) might increase GSK3β phosphorylation at serine 9 and converting Alanine (A) 11 to lysine (K) 11 might further increase GSK3β phosphorylation at serine 9 following butyric acid treatment (Fig. 5g–j). On the other hand, inserting serine (S) 13 to lysine (K)13 might have less effect on GSK3β phosphorylation at serine 9 than K15R/A11K following butyric acid treatment (Fig. 5g–j). These data suggest that K15 is a critical acetylation site in regulating the phosphorylation of GSK3β at serine 9. Moreover, the distance between serine 9 and the next lysine (11 versus 13) may play a critical role in regulating phosphorylation of GSK3β at serine 9, pending further confirmative studies. This information could contribute to a better understanding of the role of butyric acid in regulating AD pathogenesis, including that lysine (K) 15 of GSK3β is a critical acetylation site in increasing phosphorylation of GSK3β at serine 9 following treatment of butyric acid, which then leads to decreases in Tau phosphorylation and mitigation of cognitive impairment (Fig. 5k).

Treatment with *Lactobacillus* plus *Bifidobacterium* attenuated the behavioral and cellular changes in the ADWT mice

Given that ADWT mice acquired gut microbiota dysbiosis, e.g., decreased abundance of *Lactobacillus* compared to that of WT mice and *Lactobacillus and Bifidobacterium* were highly associated in the mice (Fig. 3), next we asked whether the treatment with *Lactobacillus* plus Bifidobacterium could attenuate the changes in the ADWT mice. We found that treatment with *Lactobacillus* and *Bifidobacterium* was associated with higher

amounts of butyric acid (Fig. 6a), as well as lower levels of Tau-pS202/pT205 and Tau-pS199 (Fig. 6b); less IL-6 levels (Fig. 6c); and less Aβ42 and Aβ40 amounts (Fig. 6d) in brain tissues compared to saline treatment in the ADWT mice. Additionally, the ADWT mice treated with *Lactobacillus* and *Bifidobacterium* showed improved cognitive function to those treated with saline (Fig. 6e–h and S-Fig. 9). These data suggest that treatment with *Lactobacillus* and *Bifidobacterium* may have therapeutic benefits for ADWT mice and that the gut microbiota dysbiosis observed in ADWT mice may contribute, at least partially, to the observed development of AD pathogenesis and cognitive impairment in the ADWT mice (Fig. 6i).

Partners of AD patients developed AD-associated gut microbiota dysbiosis

Finally, we determined the clinical relevance of these preclinical findings. We compared the oral and fecal microbiota profile among AD patients, partners of AD patients (PAD, living in the same household), and non-AD control (CON, without living with AD patients) (Fig. 7a and S-Fig. 10). The clinical covariates were presented in detail in S-Tables 2, 3, and S-Figs. 11, 12.

The oral microbiome analysis showed the average taxonomic distribution in AD and PAD were similar in microbial compositions with higher abundances of *Bacilli* and *Clostridia*, but lower abundances in *Gammaproteobacteria* and *Betaproteobactia* compared to CON (Fig. 7b) at the orders levels. The MaAsLin2 model demonstrated the top nine oral bacteria the abundances of which were similar between PAD and AD, but different between PAD and CON (Fig. 7c) at the species levels. Additionally, the fecal microbiome analysis revealed that the average taxonomic distribution in AD and PAD was similar, including higher levels of fecal *Lactobacillaes* but lower levels of fecal *Enterobacteriales* (Fig. 7d) compared to CON, at the orders levels. The fecal microbiota community in the AD and PAD was similar with the decreases in the abundance of *Bacteroides uniforms*, which are involved in fiber and lipid metabolic and immune system [63, 64], compared to CON (Fig. 7e). The opportunistic pathobiont *Bilophila wadsworthia* [65] and *Parabacteroides distasonis* [66] were also found to be similar between AD and PAD groups but different between CON and PAD (Fig. 7e). The oral microbiota profile in PAD was different from fecal microbiota profile in PAD (Fig. 7b, c versus Fig. 7d, e).

Furthermore, the ratio of fecal butyric acid to total SCFAs was lower, while the ratio of fecal acetic acid to total SCFAs was higher in AD and PAD compared to CON (Fig. 7f). However, despite this similarity in GMB between AD and PAD, the PAD did not show significant differences in Mini-mental state exam (MMSE) scores and clinical dementia rating (CDR) compared to the CON (S-Tables 2 and 3).

DISCUSSION

We discovered that the WT mice co-housed with AD Tg mice for 3 months, refereed as ADWT mice, developed gut microbiota dysbiosis, which resulted in the development of AD pathogenesis and cognitive impairment in the ADWT mice. The clinical findings also indicated that partners of AD patients experienced gut microbiota profile similar to that of AD patients but different from that of non-AD control. Although further investigation is

required to validate these findings, the data suggests the potential transmission of GMB from AD to non-AD individuals and the associated changes consistent with AD pathogenesis or cognitive impairment in mice. Pending further investigation, the underlying mechanism behind this GMB transmission-associated cognitive impairment may involve butyric acid, a short-chain fatty acid produced by GMB, which could impact acetylation-regulated phosphorylation of GSK3β. These changes in GSK3β may contribute to the phosphorylation of Tau protein and the subsequent cognitive impairment in the ADWT mice.

Clinical studies have reported that spouses of AD patients have a higher risk of developing incidental dementia [28–33]. Consistently, we demonstrated that the WT mice co-housed with AD Tg mice developed long time cognitive impairment (Fig. 1). Notably, the developed cognitive impairment was not due to the location or air exchange (S-Figs. 5 and 6). The accelerated time course in developing cognitive impairment in the WT mice by receiving feces from AD Tg was likely due to larger amounts of bacteria introduced to the WT mice through the gavage feeding than they would obtain by feces-eating during the co-housing (Fig. 2). Notably, the control condition of AD FMT was saline in our study, because treatment with saline is more clinically relevant and we found that there was no significant difference between saline and heat-killed bacteria in cognitive function in the mice (data not shown).

Significantly, in this study, WT mice that were co-housed with AD Tg mice for a period of 3 months developed behavioral changes at 5 months of age (Fig. 1). Conversely, WT mice co-housed with AD Tg mice for 1 month did not show behavioral changes at 3 months of age (S-Fig. 2). These findings suggest that both the duration of co-housing and the age of the mice contribute to the observed cognitive impairment. Notably, WT mice that received fecal microbiota transplantation (FMT) from AD Tg mice also developed cognitive impairment at 3 months of age. Nevertheless, further investigations are warranted to systematically compare the effects of age and duration of co-housing on cognitive function in mice in future studies.

Our mechanistic studies showed that the ADWT mice acquired gut microbiota dysbiosis and developed AD-associated pathogenesis, including increased Tau phosphorylation, IL-6 amounts, and Aβ accumulation (Fig. 4). The GMB-generated metabolites can promote metabolic benefits via the microbiota-gut-brain axis [67]. Previous studies report that SCFAs were decreased in the feces and brain of APP/PS1 mice compared to WT mice [24]. SCFAs can modulate Aβ plaques in the brain [49], astrocytic gene expression [68], expression of tight junction proteins [69], directly act on afferent vagal fibers [70], and induce ApoE-associated Tauopathy [71]. In our study, butyric acid, one of the SCFAs, decreased in AD Tg and the ADWT mice compared to WT mice both in feces and brain tissues of mice (Fig. 3v and Fig. 4a). Meanwhile, the ratio of fecal butyric acid to fecal SCFAs also decreased in AD and PAD compared to CON in clinical investigation (Fig. 7f).

Butyric acid is known to have several beneficial effects on the central nervous system, including anti-inflammatory [72] and neuroprotective effects [73]. Our studies showed that butyric acid may play a role in the acetylation-regulated phosphorylation of GSK3β, leading to Tau phosphorylation. Acetylation and phosphorylation are two types of post-translational

modifications that can impact the activity of enzymes, including kinases like GSK3β. Butyric acid has been shown to enhance acetylation and reduce phosphorylation of GSK3β, which can alter its activity and impact cellular processes [52]. Previous studies have reported that if GSK3β is acetylated at lysine (K) 183, it could decrease ability of GSK3β to phosphorylate its substrates [52]. Our studies identified that lysine (K) 15 could also be a critical acetylation site for regulating phosphorylation of GSK3β at serine 9 and the distance between serine 9 and the next lysine (K) (e.g., 11 K versus 13 K) may play a critical role in regulating the phosphorylation of GSK3β at serine 9, pending further confirmative studies. As the inhibitor of histone deacetylase (HDAC), butyric acid could modify the acetylation site at K15 and decrease the ability of GSK3β to phosphorylate its substrates including Tau (as shown in Fig. 5K). It should be noted that microbiota have the capability to generate other metabolites, beyond butyric acid [67]. Therefore, future studies will also encompass the exploration of the effects of other microbiota-derived metabolites on the pathogenesis of AD.

Replenishment GMB with *Lactobacillus* and *Bifidobacterium* prevented the reduction of butyric acid in the ADWT mice (Fig. 6a). These findings further suggest that AD-associated gut microbiota dysbiosis could reduce the amount of butyric acid, leading to Tau phosphorylation and cognitive impairment (Fig. 6i).

Germ-free mice were not used in this study because their lack of microorganisms can affect various physiological processes, including peripheral and central immune development [68], neurotransmission [74], and neurogenesis [75], which could potentially confound the study's results. Instead, AD Tg mice were co-housed with WT mice, which more closely mimics the social interactions and microorganism exchange between AD patients and their caregivers or partners that occur in a natural setting, thus leading to more clinically relevant findings in the present study.

We deliberately used male AD Tg mice and female WT mice to generate the AD Tg mice for the present study, avoiding any potential maternal transmission of AD-associated GMB from an AD mother to the next generation, as reported in previous studies [76–79], which could serve as confounding influence. Additionally, we did not use littermates of the AD Tg mice because they would have experienced same co-housing conditions as to the ADWT mice in this study, which could have introduced confounding variables into the results.

We did not find significant evidence of mucosal damage, changes in tight junction composition or structure in the small intestine or colon of AD Tg mice (S-Fig. 8). Therefore, it is unlikely that loss of gut barrier [80, 81] contributes to the changes observed in the AD Tg mice or ADWT mice in our study. Instead, we propose that the alterations in butyric acid, which can move through the gut barrier freely, are responsible for the observed changes. To test this hypothesis further, future studies should include additional experiments.

Previous studies have reported the possibility of microbiota being transmissible among family members and social network [82, 83], and the caregivers or partners of individuals of AD patients may experience changes in their microbiota due to the stress associated with caregiving [29, 30, 33]. These changes may contribute to symptoms of depression and

other associated health problems [84]. Chen et al. found that co-housing young AD Tg mice with aged AD Tg mice led to the acquisition of a similar GMB profile as that of the aged AD Tg mice, resulting in earlier onset of cognitive impairment in the young AD Tg mice [15]. Valles-Colomer et al. demonstrated person-to-person transmission of the gut and oral microbiomes [85]. In contrast to these studies, our work specifically demonstrated that GMB could be transmitted from AD Tg mice to WT mice. Our results also illustrated that the WT mice co-housed with AD Tg mice acquired AD-associated gut microbiota dysbiosis, leading to the development of AD pathogenesis and cognitive impairment (Figs. 1, 2 and 3). This co-housing mouse model more closely approximates the clinical condition where partners (e.g., spouses) of AD patients co-habit with AD patients. Importantly, our study showed that feces exchange via co-housing, rather than airborne transmission or environmental conditions, was associated with the cognitive impairment (S-Figs. 5 and 6). Finally, we demonstrated that AD patients could transmit oral and gut microbiota to their non-AD partners (Fig. 7).

The microbiota profile of ADWT mice differed from that of PAD, indicating species-specific differences in the microbiota. Mice and humans have distinct evolutionary histories and physiological variances, leading to variations in their gut microbiota composition [86]. As a result, the microbial communities that naturally inhabit the mouse gut are distinct from those found in humans.

Interestingly, certain WT mice that received FMT did not exhibit cognitive impairment as detected in the BM test (Fig. 2), suggesting the possible presence of two subpopulations with varying cognitive function. The exact reason for this observation remains unknown at present. We can speculate on three potential explanations. Firstly, it is possible that the WT mice that did not experience cognitive impairment following the administration of FMT from AD Tg mice might not have received a sufficient quantity of FMT. Secondly, these differences in cognitive function could be attributed to inherent behavioral variabilities among the mice. Lastly, it is possible that certain WT mice were not responsive or sensitive to the effects of FMT derived from AD Tg mice. In future investigations, we intend to utilize the established system described in this study to further explore the impact of FMT from AD Tg mice on cognitive function in WT mice.

Feces obtained from 3-month-old 5XFAD mice, a transgenic model of AD, were administered to WT mice with the aim of inducing cognitive impairment. Notably, 5XFAD mice may exhibit evident AD pathogenesis by the age of 3 months [87]. Consequently, it is logical to expect that WT mice receiving FMT from the 3-month-old 5XFAD mice would also develop cognitive impairment. These findings strongly suggest the potential transmission of gut microbiota from AD Tg mice to WT mice, leading to cognitive impairment. However, further confirmatory investigations are warranted to support these observations.

The present study has some limitations that should be acknowledged. First, despite co-housing AD Tg mice with WT mice, we did not observe any cognitive improvement in the AD Tg mice (S-Fig. 3). This is in contrast to the WT mice, which exhibited cognitive impairment when co-housed with AD Tg mice (Fig. 1). The exact reason for this discrepancy remains unclear; however, it is possible that the 5XFAD mice utilized in

our study had already developed an aggressive form of AD pathogenesis. Consequently, their cognitive impairment may have been beyond recovery through the transmission of GMB from WT mice. To further investigate whether co-housing with WT mice can enhance cognitive function in AD Tg mice, future studies could consider employing less aggressive AD Tg mouse models, such as the APP Tg2576 model [88]. Second, in the present study, we exclusively used female mice due to the observed tendency of male AD Tg and WT mice to engage in fighting when co-housed. This precaution was taken to prevent any potential confounding of the results that could arise from such fighting behavior. Third, the in vitro studies involving butyric acid were conducted using HEK 293T cells instead of primary neurons. The use of HEK 293T cells allowed us to establish the system and generate initial hypotheses. However, we acknowledge the importance of studying butyric acid in primary neurons, and we plan to repeat the in vitro experiments using primary neurons in future investigations, utilizing the established system as a foundation. Finally, although we observed a partial transfer of oral and fecal microbiota from AD patients to PAD, the PAD did not develop cognitive impairment, while ADWT mice developed cognitive impairment. The exact reason of such difference is not known at present. One possible explanation for this discrepancy could be that the AD and PAD individuals did not co-habit long enough for the PAD individuals to develop incidental AD dementia. Our animal studies support this hypothesis, as short-term co-housing (1 month) between AD Tg mice and WT mice did not result in cognitive impairment in the WT mice. Furthermore, it is important to consider that the increased risk of incidental dementia observed in partners of AD patients can be attributed to various factors, such as diet, stress, and age. Although the current study revealed a partial transfer of gut and oral microbiota from AD patients to their partners (PAD), it is noteworthy that the PAD did not exhibit cognitive impairment. This intriguing finding necessitates further investigation in future studies to better understand the implications and potential impact of microbiota on cognitive function in patients.

In conclusion, this initial proof-of-concept study demonstrated the potential transmission of microbiota from AD patients or AD Tg mice to non-AD controls or WT mice housed together. This transmission may contribute to the development of AD-associated microbiota dysbiosis and metabolite alterations, ultimately leading to AD pathogenesis and cognitive impairment. However, these findings should be validated in future studies. The results of this study are expected to drive further research to explore gut microbiota dysbiosis and its connection to AD in both preclinical and clinical contexts.

MATERIALS AND METHODS

The Standing Committee on Animals at Mass General Brigham (MGB), Boston, MA (Protocol number: 2006N000219) approved the animal protocol. We performed all experiments according to the National Institutes of Health guidelines and regulations. We made every effort to minimize the number of animals used. We wrote the manuscript according to ARRIVE guidelines.

Mice, bacterial and cell strains

AD Tg mice [B6SJL-Tg (APPSwFlLon, PSEN1*M146L*L286V) 6799Vas/Mmjax, Stock No. 34848-JAX, Jackson Lab, Bar Harbor, ME] and WT mice (C57BL/6J, Jackson Lab) were used in the present studies. We bred and maintained the AD Tg (5XFAD) mice in our own animal facilities, typically using male AD Tg mice with female WT mice to generate the AD Tg mice confirmed by genotyping. We employed *Lactobacillus reuteri* [American Type Culture Collection (ATCC), Manassas, VA, Dsm 20016 *Lactobacillus reuteri* (53609)], *Bifidobacterium pseudolongum* (ATCC, Manassas, VA, Catalog 25526), and HEK 293T cell (Cat# CRL-3216; ATCC, RRID: CVCL_0063) in the studies.

Co-housing of AD Tg mice with WT mice to generate the ADWT mice

To generate ADWT mice, 2-month-old female AD Tg mice were co-housed with age-matched female WT mice for 3 months. The WT mice co-housed with AD Tg mice for 1 month was not referred as ADWT mice. The mice were maintained in a non-germ-free facility with a 12:12 h light: dark cycle (lights on at 7:00 a.m.), and ad libitum access to food and water, mimicking real-world conditions. Each cage housed two AD Tg mice [B6SJL-Tg (APPSwFlLon, PSEN1*M146L*L286V) 6799Vas/Mmjax, Stock No. 34848-JAX, Jackson Lab, Bar Harbor, ME] and two WT mice (C57BL/6J, Jackson Lab). After the separation, four ADWT mice were housed in one cage for subsequent studies. These ADWT mice, which could possess some AD-associated gut microbiota and pathogenesis, are not AD Tg mice, and conceptually represent the non-AD population in animal research.

Air exchange between AD Tg mice and WT mice

To investigate whether cognitive changes were specifically due to co-housing and not via air exchange, we conducted an experiment where the cage containing four AD Tg mice and the cage containing four WT mice were placed side-by-side to allow air exchange between the two cages without physical contact between the AD Tg mice and the WT mice. This experiment was designed to separate the effects of co-housing from potential confounding factors such as air exchange. We then determined the cognitive function of the WT mice.

Different locations of cages

To evaluate the effect of location on cognitive function in WT mice, we conducted an experiment where cages containing four WT mice were placed in different rooms. This was done to rule out any potential location confounds that may affect the cognitive function of the mice. We then determined the cognitive function of these WT mice.

Microbiota transplantation

Female wild-type mice at 2 months of age were randomly assigned to two groups (ten mice in each group), and received a cocktail of four antibiotics (ampicillin, vancomycin, neomycin, and metronidazole) in their drinking water for one week as described before [89]. After the antibiotic treatment, each mouse was administrated by gavage with 0.2 mL of a suspension of fecal material obtained from either 3-month-old AD Tg mice or age-matched WT mice. Fecal samples were prepared as described previously [90, 91], and each mouse received daily treatment for 7 days. Control mice received only saline for the same duration.

One month after the last gavage, cognitive function was assessed using the Morris water maze and Barnes maze.

Morris water maze

The Morris water maze (MWM) test was conducted following previously established protocols [92]. Briefly, mice were subjected to four trials per day for 7 consecutive days in the MWM starting at one day after the end of co-housing. Escape latency, the time taken to reach the platform, was recorded in each trial to assess learning function, and the average escape latency from the four trials was calculated and analyzed each day. On the final day, the platform was removed, and the number of platform crossings was counted to measure memory function. Swimming speed was also recorded and analyzed. Mice were kept warm using a heating device throughout the experiment.

Barnes maze

The same group of mice were tested in the Barnes maze (BM) one day after completing the MWM test, following the previously established methods [93]. The BM training included two trials per day (3 min per trial with 15-minute intervals) for four consecutive days. During BM training, the latency to identify and enter the escape box was measured and recorded for each mouse. Five days after BM training, BM testing was conducted to record and measure the latency to identify and enter the escape box, the number of wrong holes searched, distance traveled, and time spent in the target zone. The testing was initiated by placing a mouse under a bucket in the center of the circular platform and using bright light (200 W) and noise (85 decibels) to stimulate escape behavior. If the mouse did not enter the escape box within three minutes of the stimulation, it was gently guided to the correct hole. The buzzer was turned off immediately when the mouse entered the tunnel connecting the hole and the escape box. Each mouse was allowed to remain in the escape box for 1 min before being returned to the home cage. Latency to identify and enter the escape box and speed were recorded during BM training, while latency, target zone entrances, wrong holes searched, distance, and speed were measured during BM testing.

Gavage with lactobacillus and bifidobacterium in mice

Lactobacillus reuteri [American Type Culture Collection (ATCC), Manassas, Virginia, Catalog 53609] were cultured in ATCC medium (78 Lactobacillus medium) at 37 °C in an aerobic environment, composed of 20 g/L tryptone, 5 g/L tryptose, 5 g/L yeast extract, 200 ml/L tomato juice, 1 g/L liver extract concentrate, 0.05 g/L Tween 80, 3 g/L glucose, and 2 g/L lactose (pH 6.5). *Bifidobacterium pseudolongum* (ATCC, Catalog 25526) were cultured in ATCC Medium (2107) at 37 °C in an anaerobic environment. The medium was composed of 10 g/L tryptose, 10 g/L beef extract, 3 g/L yeast extract, 5 g/L dextrose, 5 g/L NaCl, 1 g/L soluble starch, 0.5 g/L L-cysteine HCl, 3 g/L sodium acetate, and 4 ml/L resazurin (0.025%) (pH 6.8). For the first 10 days of each month during the 3-month co-housing with the AD Tg mice, each ADWT mouse received either 10^9 CFU *Lactobacillus reuteri* plus *Bifidobacterium pseudolongum* (10^9 CFU in 200 μL of saline) or saline by gavage once per day.

Collection of mice feces and harvest of brain tissues of mice

At the end of co-housing for three months, fecal samples were collected from each mouse in the study (N = 6–12 in each group). Additionally, cortex and hippocampus were harvested from each mouse at the end of the last behavioral test.

DNA extraction and 16S rRNA gene sequencing

We collected fecal samples from the mice, and fecal and oral samples from human participants and stored them at −80 °C until being shipped for analysis. The 16S rRNA gene sequencing was performed by BGI America (Cambridge, MA, for mouse samples) or BGI China (Shanghai, PR China, for human samples) using the manufacturer's protocol, following previously established procedures [93]. In brief, mouse fecal samples were placed in 1.5 ml tubes, snap-frozen on dry ice, and stored at −80 °C until being shipped on dry ice for analysis. In the clinical investigation, participants were asked to provide a fecal and oral sample whenever they were ready. Samples were taken in fecal and oral collection containers, then transferred on ice and stored at −80 °C in tubes supplied with OmniGene Gut kits (OMR-200, DNA Genotek, OraSure Technologies, Bethlehem, PA) until DNA extraction.

Quantification of fecal SCFAs

Quantification of fecal SCFAs was performed as previously described [94]. Briefly, fecal samples were homogenized, and their dry weight was determined. The homogenates were then diluted and stored at −80 °C. To quantify SCFAs, an aliquot of the homogenate was centrifuged, and the clear supernatant was collected. The pH of the supernatant was adjusted to 2–3 using 5 M HCl, and the suspension was centrifuged again. The clear supernatant was transferred to a new tube, and an internal standard (2-ethylbutyric acid) was added. SCFA quantification was performed by gas chromatography using a Shimadzu GC-2014 system with a fused-silica capillary column and a free fatty acid phase. The flow rates for hydrogen, air, and nitrogen were 30, 300, and 20 mL/min, respectively, and the injected sample volume was 1 μL. We quantified eight SCFAs: acetic acid, propionic acid, butyric acid, isobutyric acid, valeric acid, isovaleric acid, hexanoic acid, and 2-ethylbutyric acid (internal standard).

Quantification of brain SCFAs

Quantification of brain SCFAs was performed as previously described [95]. Briefly, the method involves homogenizing 0.1 gram of the tissue in 500 μl of aqueous acetonitrile and extracting the supernatant with 8 ml of extraction buffer (hexane: diethyl ether = 1:1). After centrifugation, 7.5 ml of the supernatant was collected and mixed with 93 μl of 20 mM KOH in methanol, and then dried at 40 °C under nitrogen gas. The dried residue is reconstituted in 50 μl of 2.5% 18-Crown-6 in acetonitrile and is further derivatized with 9-chloromethylanthracene in acetonitrile with the addition of tetramethylammonium hydroxide. The derivatized sample is loaded onto an Acclaim C18 column (3 μm, 4.6 × 100 mm, ThermoFisher Scientific, Waltham, MA) and separated using an Ultimate 3000 high-performance liquid chromatograph (HPLC, ThermoFisher Scientific) equipped with a UV-visible detector. 2-ethylbutyric acid was added as an internal reference control, and the peak area of SCFAs was measured. The peak area of each sample is normalized with that of

2-ethylbutyric acid in the sample, and the results were presented as ratios of SCFAs in the treatment group to the control group.

Enzyme-linked immunosorbent assays (ELISA)

The immunoassay kits used to detect IL-6, Aβ42, Aβ40, and Tau-pS199 in mouse brain tissue were: Mouse IL-6 immunoassay kit (Catalog number: M6000B, R&D Systems, Minneapolis, MN); Mouse Aβ42 ELISA kit (Catalog number: KHB3441, Invitrogen); Mouse Aβ40 ELISA kit (Catalog number: KHB3481, Invitrogen), and mouse Tau (Phospho) [Tau-pS199] ELISA Kit (Catalog number: KMB7041, Invitrogen). The manufacturer's instructions were followed for each kit to determine the amount of IL-6, Aβ42, Aβ40, and Tau-pS199 in mouse brain tissue, respectively. The optical density of each well was measured at 450 nm and corrected at 570 nm, as described in a previous study [92].

Western blot analysis

Western blot analysis was performed as previously described [96]. We used the following antibodies: AT8 (55 kDa, 1:1000, Invitrogen, Carlsbad, CA) to detect Tau phosphorylated at serine 202 (Tau-pS202) and threonine 205 (Tau-pT205); anti-Tau (phospho S262) (55 kDa, 1:1,000, Abcam, Cambridge, MA, ab131354) to detect Tau phosphorylated at serine 262 (Tau-pS262); Tau antibody (ab254256, Abcam, Cambridge, MA, 1:1000) to detect total Tau; GSK3α/β antibody (1:1000, 52 kDa, Cell Signaling Technology, Danvers, MA) to detect total GSK3β; and p-GSK3βS9 antibody (1:1000, 52 kDa, Cell Signaling Technology) to detect GSK3β phosphorylated at serine 9. Both β-Actin antibody (1:5000, 42 kDa, Sigma, St. Louis, MO) and GAPDH antibody (1:5000, 36 kDa, Cell Signaling Technology, Danvers, MA) were used to detect β-actin and GAPDH, respectively, as the loading control. The signal intensity was analyzed using a Bio-Rad (Hercules, CA) image program, and the changes in protein amounts were presented as a percentage of those in control mice, where a protein level of 100% indicates control levels.

Cell culture and butyric acid treatment

HEK 293T cells (CRL-3216, ATCC) were cultured in Dulbecco's modified Eagle's medium (DMEM) with high glucose, supplemented with 5% heat-inactivated fetal calf serum, 100 U/ml penicillin, 100 μg/ml streptomycin, and 2 mM L-glutamine. One million cells were seeded in 100 × 20 mm dishes with 10 ml of cell culture media and incubated overnight. The sodium butyrate (butyric acid) (Sigma, St. Louis, MO) was prepared as a 1 M stock solution in ultrapure deionized water and freshly diluted with culture medium to final treatment concentrations of 0, 5, 10, or 20 mM. The cells were then used for treatment with butyric acid, site-mutation, Western blot analysis or mass spectrometry studies.

Mass spectrometry (MS) study

The HEK 293T cells were harvested for protein analysis by using immunoprecipitation (IP) and mass spectrometry (MS) as previously described [97] at the Taplin Mass Spectrometry Facility of Harvard Medical School, Boston, MA. First, the cells were washed with ice-cold DPBS buffer and lysed using ice-cold IP lysis buffer containing protease and phosphatase inhibitors. The lysate was centrifuged to remove cell debris, and the supernatant was mixed

with protein A/G beads for pre-cleaning. The pre-cleared lysate was then incubated with specific antibody [GSK3α/β (1:1000, 52 kDa, Cell Signaling Technology)] and fresh beads overnight at 4 °C. The antibody-bound beads were washed with IP buffer and the mixture of beads and SDS sample buffer were heated at 95 °C for 10 minutes. The protein samples were separated by SDS-PAGE, and the desired protein bands were excised from the gel. The gel pieces were destained using 100 mM ammonium bicarbonate (pH 8.9) in 50% acetonitrile, and the protein content was analyzed using mass spectrometry.

Plasmid constructs and transfection

The mammalian expression plasmid for GSK3β WT in pcDNA3 (Plasmid # 14753) was obtained from Addgene (Watertown, MA), while site-directed mutants were created using the GeneArt® Site-Directed Mutagenesis System (A13282, ThermoFisher Scientific) and standard molecular biology techniques. All constructs were confirmed by Sanger sequencing, and a complete list of primers was provided, including 15 R (sense-5′cctttgcggagagctgcaggccggtgcagcagcctt3′; anti-sense-5′aaggctgctgcaccggcctgcagctctccgcaaagg3′), 11K/15R (sense-5′agaaccacctcctttaaggagagctgcaggccggtg3′; anti-sense-5′caccggcctgcagctctccttaaaggaggtggttct3′), and 13K/15 R (sens e-5′acctcctttgcggagaagtgcaggccggtgcagcag3′; anti-sense-5′ctgctgcaccggcctgcacttctccgcaaaggaggt3). The plasmids were then transiently transfected into HEK 293T cells (CRL-3216, ATCC) using Lipofectamine 3000 reagents (Invitrogen) following the manufacturer's instructions.

Immune staining and morphometry

Formalin-fixed paraffin-embedded (FFPE) analysis was performed as previously described [80, 81]. Briefly, the colon and small intestine samples were processed as swiss rolls and baked at 60 °C overnight. To prepare for the tissue sections for immunofluorescence staining, heat-assisted deparaffinization, rehydration, and antigen retrieval were carried out using Tinto-Deparaffinatior Citrate (BioSB, Santa Barbara, CA). To minimize tissue autofluorescence, the sections were then incubated for 2 h in bleaching buffer under broad spectrum LED light. After blocking with Serum Free Protein Block (Agilent, Santa Barbara, CA), the sections were incubated with primary antibodies and incubated for 8 h at room temperature. Following washing, the sections were incubated with secondary antibodies and Hoechst 33342 (1 μg/ml), and then mounted with Slow-fade (ThermoFisher scientific; cat# S36963). The tissue samples were imaged using a DM4000 microscope with a 20× NA 0.7 HC PLAN APO objective (Leica), multichannel dichroic and single band emission filters (Semrock, Rochester, NY), Aura light engine (Lumencor, Beaverton, OR), and ORCA-Flash 4.0 LT+ camera (Hamamatsu Photonics, Shizuoka, Japan), controlled by Metamorph 7.8 (Molecular Devices, San Jose, CA). Hematoxylin and eosin (H & E) stained sections were also imaged using a transmitted white LED light source and MicroPublisher 5.0 camera (Q Imaging, British Columbia, Canada). Quantitative immunostain analyses were conducted using Cell Profiler software developed by the Broad Institute. The nuclei labeled with Hoechst 33342 were used to identify the tissue, and the epithelial mask was generated based on the E-cadherin signal. The E-cadherin staining was also used to create masks that demarcated the basolateral membranes for the analysis of claudin-4. Tight junction

masks generated based on ZO-1 labeling were used to analyze the expression of claudin-2, occludin, and ZO-1. Prior to the analysis, the consistency of E-cadherin staining across samples was validated, and E-cadherin was used to normalize the signal intensity.

Human study design and participants

The study protocol was approved by the Human Research Ethics Committee of the Shanghai Tenth People's Hospital, and all participants or family members provided written informed consent before enrollment. The study was registered on ClinicalTrials.gov (NCT03827733). We conducted a cross-sectional cohort study in Shanghai, China from October 2017 to December 2019. A total of 157 participants were initially screened for the study, including AD patients, partners of AD patients, and normal controls. To be eligible, participants had to be at least 50 years old, with five or more years of education, normal vision and hearing, and speaking Chinese Mandarin. Exclusion criteria included prior neurologic or gastrointestinal disease, mental disorders, recent (e.g., one week) use of antibiotics, and unwillingness to comply with cognitive assessments. AD patients were defined based on clinical diagnosis, MMSE score, CDR, ADL score, and Hachinski Ischemia scale score [98]. Participants in the control group had MMSE scores of at least 24 and CDRs of zero. Of the 157 participants screened, 49 were excluded for various reasons, and 108 participants were included in the data analysis, with fecal samples collected from 94 of them. The fecal and oral samples were collected at different times of the day, coinciding with participants' bowel movements and the discharge of feces. The collection of fecal and oral samples was not possible for every participant due to technical reasons and/or willingness.

Study size estimation

The objective of the present study was to assess potential differences in microbiota of AD, PAD and control (CON) participants. Based on prior experience, we aimed to recruit at least 20 participants in AD, PAD, or CON participants in this exploratory study.

Statistics

Data were expressed as means ± standard deviations (SD) or medians and interquartile ranges (25–75%). Data were first tested for normality for behavioral and biochemical studies using the Shapiro–Wilk test. Data with normal distributions were analyzed by Student's *t*-test, one-way ANOVA, or two-way ANOVA with post hoc analyses (Bonferroni comparison). The Mann–Whitney *U* test analyzed data with abnormal distributions. The Microbiome Analysis Core at the Harvard T.H. Chan School of Public Health (Microbiome Analysis Core), Boston, MA analyzed the human and mice microbiota data. Microbiome Multivariable Association with Linear (MaAsLin2) implementation was used for tests in microbiome profiles taxonomic result as described in a previous study [53]. Univariate statistical tests included Student's *t*-test (for normally distributed data according to the Shapiro–Wilk *W* test) or Mann–Whitney–Wilcoxon test (MWW, for non-normal distributions) for binary comparisons; analysis of variance (ANOVA, for normal distributions), or Kruskal–Wallis–Wilcoxon (KWW, for non-normal distributions) for ternary comparisons. Multivariate analyses included principal component analysis and partial least squares discriminator analysis. Outliers, determined by Jackknife distance analysis, were removed from further analysis. *P* values < 0.05 were considered statistically

significant. We used prism 9 software (Graph Pad Software) and JMP Pro 14 (Cary, NC) to analyze the data.

Reporting summary

The paper's raw sequence data has been deposited in the Genome Sequence Archive and is publicly accessible at https://www.ncbi.nlm.nih.gov/sra/PRJNA991622, https://www.ncbi.nlm.nih.gov/sra/PRJNA992485, https://www.ncbi.nlm.nih.gov/sra/PRJNA991093. The accession number for the data has been deposited in accordance with the guidelines set out by Genomics, Proteomics & Bioinformatics in 2021 and Nucleic Acids Res in 2022. This information is essential for anyone wishing to access or use the data for further research or analysis. Simplesubmission.com performed the submission of the raw sequence data.

Supplementary Material

Refer to Web version on PubMed Central for supplementary material.

ACKNOWLEDGEMENTS

We gratefully acknowledge the funding support for this study provided by the National Institutes of Health through R01AG041274, R01AG062509, and RF1070761, and Henry L. Beecher Professorship from Harvard University (awarded to Zhongcong Xie), and R21AG065606 (awarded to Yiying Zhang). The GMB analyses presented in this paper were partially conducted at the Harvard Chan Microbiome Analysis Core, located at the Harvard Public Health School, Boston, MA. We also acknowledge Dr. Jackie Washington and Dr. Zhiyi Zuo from University of Virginia for conducting the Brain SCFAs analysis. We would like to thank Dr. Yang Shi of Ludwig Cancer Research at the University of Oxford for his valuable comments and insightful discussions.

DATA AVAILABILITY

All data are available in the main text or the supplementary materials. The source data can be available from the corresponding authors on reasonable request.

REFERENCES

1. Nianogo RA, Rosenwohl-Mack A, Yaffe K, Carrasco A, Hoffmann CM, Barnes DE. Risk factors associated with Alzheimer disease and related dementias by sex and race and ethnicity in the US. JAMA Neurol. 2022;79:584–91. [PubMed: 35532912]
2. Selkoe DJ. Alzheimer's disease: genes, proteins, and therapy. Physiol Rev. 2001;81:741–66. [PubMed: 11274343]
3. Grundke-Iqbal I, Iqbal K, Quinlan M, Tung YC, Zaidi MS, Wisniewski HM. Microtubule-associated protein tau. A component of Alzheimer paired helical filaments. J Biol Chem. 1986;261:6084–9. [PubMed: 3084478]
4. Grundke-Iqbal I, Iqbal K, Tung YC, Quinlan M, Wisniewski HM, Binder LI. Abnormal phosphorylation of the microtubule-associated protein tau (tau) in Alzheimer cytoskeletal pathology. Proc Natl Acad Sci USA. 1986;83:4913–7. [PubMed: 3088567]
5. Trojanowski JQ, Lee VM. Paired helical filament tau in Alzheimer's disease. The kinase connection. Am J Pathol. 1994;144:449–53. [PubMed: 8129030]
6. Buee L, Bussiere T, Buee-Scherrer V, Delacourte A, Hof PR. Tau protein isoforms, phosphorylation and role in neurodegenerative disorders. Brain Res Brain Res Rev. 2000;33:95–130. [PubMed: 10967355]
7. Holtzman DM, Carrillo MC, Hendrix JA, Bain LJ, Catafau AM, Gault LM, et al. Tau from research to clinical development. Alzheimers Dement. 2016;12:1033–9. [PubMed: 27154059]

8. Wang Y, Mandelkow E. Tau in physiology and pathology. Nat Rev Neurosci. 2016;17:5–21. [PubMed: 26631930]
9. Heneka MT, Carson MJ, El Khoury J, Landreth GE, Brosseron F, Feinstein DL, et al. Neuroinflammation in Alzheimer's disease. Lancet Neurol. 2015;14:388–405. [PubMed: 25792098]
10. Calsolaro V, Edison P. Neuroinflammation in Alzheimer's disease: current evidence and future directions. Alzheimers Dement. 2016;12:719–32. [PubMed: 27179961]
11. Long JM, Holtzman DM. Alzheimer disease: an update on pathobiology and treatment strategies. Cell. 2019;179:312–39. [PubMed: 31564456]
12. Long-Smith C, O'Riordan KJ, Clarke G, Stanton C, Dinan TG, Cryan JF. Microbiota-gut-brain axis: new therapeutic opportunities. Annu Rev Pharm Toxicol. 2020;60:477–502.
13. Fulling C, Dinan TG, Cryan JF. Gut microbe to brain signaling: what happens in vagus. Neuron. 2019;101:998–1002. [PubMed: 30897366]
14. Liu L, Huh JR, Shah K. Microbiota and the gut-brain-axis: Implications for new therapeutic design in the CNS. EBioMedicine. 2022;77:103908.
15. Chen C, Ahn EH, Kang SS, Liu X, Alam A, Ye K. Gut dysbiosis contributes to amyloid pathology, associated with C/EBPbeta/AEP signaling activation in Alzheimer's disease mouse model. Sci Adv. 2020;6:eaba0466.
16. Chen C, Liao J, Xia Y, Liu X, Jones R, Haran J, et al. Gut microbiota regulate Alzheimer's disease pathologies and cognitive disorders via PUFA-associated neuroinflammation. Gut. 2022;71:2233–52. [PubMed: 35017199]
17. Zhuang ZQ, Shen LL, Li WW, Fu X, Zeng F, Gui L, et al. Gut microbiota is altered in patients with Alzheimer's disease. J Alzheimers Dis. 2018;63:1337–46. [PubMed: 29758946]
18. Zhu X, Li B, Lou P, Dai T, Chen Y, Zhuge A, et al. The relationship between the gut microbiome and neurodegenerative diseases. Neurosci Bull. 2021;37:1510–22. [PubMed: 34216356]
19. Cattaneo A, Cattane N, Galluzzi S, Provasi S, Lopizzo N, Festari C, et al. Association of brain amyloidosis with pro-inflammatory gut bacterial taxa and peripheral inflammation markers in cognitively impaired elderly. Neurobiol Aging. 2017;49:60–68. [PubMed: 27776263]
20. Vogt NM, Kerby RL, Dill-McFarland KA, Harding SJ, Merluzzi AP, Johnson SC, et al. Gut microbiome alterations in Alzheimer's disease. Sci Rep. 2017;7:13537. [PubMed: 29051531]
21. Liu P, Wu L, Peng G, Han Y, Tang R, Ge J, et al. Altered microbiomes distinguish Alzheimer's disease from amnestic mild cognitive impairment and health in a Chinese cohort. Brain Behav Immun. 2019;80:633–43. [PubMed: 31063846]
22. Shen L, Liu L, Ji HF. Alzheimer's disease histological and behavioral manifestations in transgenic mice correlate with specific gut microbiome state. J Alzheimers Dis. 2017;56:385–90. [PubMed: 27911317]
23. Chen Y, Fang L, Chen S, Zhou H, Fan Y, Lin L, et al. Gut microbiome alterations precede cerebral amyloidosis and microglial pathology in a mouse model of Alzheimer's disease. Biomed Res Int. 2020;2020:8456596.
24. Zhang L, Wang Y, Xiayu X, Shi C, Chen W, Song N, et al. Altered gut microbiota in a mouse model of Alzheimer's disease. J Alzheimers Dis. 2017;60:1241–57. [PubMed: 29036812]
25. Cuervo-Zanatta D, Garcia-Mena J, Perez-Cruz C. Gut microbiota alterations and cognitive impairment are sexually dissociated in a transgenic mice model of Alzheimer's disease. J Alzheimers Dis. 2021;82:S195–S214. [PubMed: 33492296]
26. Harach T, Marungruang N, Duthilleul N, Cheatham V, Mc Coy KD, Frisoni G, et al. Reduction of Abeta amyloid pathology in APPPS1 transgenic mice in the absence of gut microbiota. Sci Rep. 2017;7:41802. [PubMed: 28176819]
27. Brandscheid C, Schuck F, Reinhardt S, Schafer KH, Pietrzik CU, Grimm M, et al. Altered gut microbiome composition and tryptic activity of the 5xFAD Alzheimer's mouse model. J Alzheimers Dis. 2017;56:775–88. [PubMed: 28035935]
28. Marriage Williams C. and mental health: when a spouse has Alzheimer's disease. Arch Psychiatr Nurs. 2011;25:220–2 [PubMed: 21621735]
29. Lee S, Kawachi I, Grodstein F. Does caregiving stress affect cognitive function in older women? J Nerv Ment Dis. 2004;192:51–7. [PubMed: 14718776]

30. Vitaliano PP, Echeverria D, Yi J, Phillips PE, Young H, Siegler IC. Psychophysiological mediators of caregiver stress and differential cognitive decline. Psychol Aging. 2005;20:402–11. [PubMed: 16248700]
31. de Vugt ME, Jolles J, van Osch L, Stevens F, Aalten P, Lousberg R, et al. Cognitive functioning in spousal caregivers of dementia patients: findings from the prospective MAASBED study. Age Ageing. 2006;35:160–6. [PubMed: 16495293]
32. Mackenzie CS, Smith MC, Hasher L, Leach L, Behl P. Cognitive functioning under stress: evidence from informal caregivers of palliative patients. J Palliat Med. 2007;10:749–58. [PubMed: 17592987]
33. Norton MC, Smith KR, Ostbye T, Tschanz JT, Corcoran C, Schwartz S, et al. Greater risk of dementia when spouse has dementia? The Cache County study. J Am Geriatr Soc. 2010;58:895–900. [PubMed: 20722820]
34. Cryan JF, Dinan TG. Mind-altering microorganisms: the impact of the gut microbiota on brain and behaviour. Nat Rev Neurosci. 2012;13:701–12. [PubMed: 22968153]
35. Ma Y, Ajnakina O, Steptoe A, Cadar D. Higher risk of dementia in English older individuals who are overweight or obese. Int J Epidemiol. 2020;49:1353–65. [PubMed: 32575116]
36. Wieckowska-Gacek A, Mietelska-Porowska A, Wydrych M, Wojda U. Western diet as a trigger of Alzheimer's disease: from metabolic syndrome and systemic inflammation to neuroinflammation and neurodegeneration. Ageing Res Rev. 2021;70:101397.
37. Grant WB. Using multicountry ecological and observational studies to determine dietary risk factors for Alzheimer's disease. J Am Coll Nutr. 2016;35:476–89. [PubMed: 27454859]
38. Yusufov M, Weyandt LL, Piryatinsky I. Alzheimer's disease and diet: a systematic review. Int J Neurosci. 2017;127:161–75. [PubMed: 26887612]
39. Musiek ES, Holtzman DM. Three dimensions of the amyloid hypothesis: time, space and 'wingmen'. Nat Neurosci. 2015;18:800–6. [PubMed: 26007213]
40. Hatfield CF, Herbert J, van Someren EJ, Hodges JR, Hastings MH. Disrupted daily activity/rest cycles in relation to daily cortisol rhythms of home-dwelling patients with early Alzheimer's dementia. Brain. 2004;127:1061–74. [PubMed: 14998915]
41. Kumar D, Koyanagi I, Carrier-Ruiz A, Vergara P, Srinivasan S, Sugaya Y, et al. Sparse activity of hippocampal adult-born neurons during REM sleep is necessary for memory consolidation. Neuron. 2020;107:552–65.e510 [PubMed: 32502462]
42. Meng Q, Lin MS, Tzeng IS. Relationship between exercise and alzheimer's disease: a narrative literature review. Front Neurosci. 2020;14:131. [PubMed: 32273835]
43. Maass A, Duzel S, Goerke M, Becke A, Sobieray U, Neumann K, et al. Vascular hippocampal plasticity after aerobic exercise in older adults. Mol Psychiatry. 2015;20:585–93. [PubMed: 25311366]
44. Chandra S, Sisodia SS, Vassar RJ. The gut microbiome in Alzheimer's disease: what we know and what remains to be explored. Mol Neurodegener. 2023;18:9. [PubMed: 36721148]
45. Minter MR, Zhang C, Leone V, Ringus DL, Zhang X, Oyler-Castrillo P, et al. Antibiotic-induced perturbations in gut microbial diversity influences neuroinflammation and amyloidosis in a murine model of Alzheimer's disease. Sci Rep. 2016;6:30028. [PubMed: 27443609]
46. Dodiya HB, Kuntz T, Shaik SM, Baufeld C, Leibowitz J, Zhang X, et al. Sex-specific effects of microbiome perturbations on cerebral Abeta amyloidosis and microglia phenotypes. J Exp Med. 2019;216:1542–60. [PubMed: 31097468]
47. Dodiya HB, Lutz HL, Weigle IQ, Patel P, Michalkiewicz J, Roman-Santiago CJ, et al. Gut microbiota-driven brain Abeta amyloidosis in mice requires microglia. J Exp Med. 2022;219:e20200895.
48. Mezo C, Dokalis N, Mossad O, Staszewski O, Neuber J, Yilmaz B, et al. Different effects of constitutive and induced microbiota modulation on microglia in a mouse model of Alzheimer's disease. Acta Neuropathol Commun. 2020;8:119. [PubMed: 32727612]
49. Colombo AV, Sadler RK, Llovera G, Singh V, Roth S, Heindl S, et al. Microbiota-derived short chain fatty acids modulate microglia and promote Abeta plaque deposition. Elife. 2021;10:e59826.

50. Dodiya HB, Frith M, Sidebottom A, Cao Y, Koval J, Chang E, et al. Synergistic depletion of gut microbial consortia, but not individual antibiotics, reduces amyloidosis in APPPS1–21 Alzheimer's transgenic mice. Sci Rep. 2020;10:8183. [PubMed: 32424118]
51. Amaral AC, Perez-Nievas BG, Siao Tick Chong M, Gonzalez-Martinez A, Argente-Escrig H, Rubio-Guerra S, et al. Isoform-selective decrease of glycogen synthase kinase-3-beta (GSK-3beta) reduces synaptic tau phosphorylation, transcellular spreading, and aggregation. iScience. 2021;24:102058.
52. Sarikhani M, Mishra S, Maity S, Kotyada C, Wolfgeher D, Gupta MP, et al. SIRT2 deacetylase regulates the activity of GSK3 isoforms independent of inhibitory phosphorylation. Elife. 2018;7:e32952.
53. Mallick H, Rahnavard A, McIver LJ, Ma S, Zhang Y, Nguyen LH, et al. Multivariable association discovery in population-scale meta-omics studies. PLoS Comput Biol. 2021;17:e1009442.
54. Westfall S, Caracci F, Estill M, Frolinger T, Shen L, Pasinetti GM. Chronic stress-induced depression and anxiety priming modulated by gut-brain-axis immunity. Front Immunol. 2021;12:670500.
55. Gungor B, Adiguzel E, Gursel I, Yilmaz B, Gursel M. Intestinal microbiota in patients with spinal cord injury. PLoS ONE. 2016;11:e0145878.
56. Qu D, Sun F, Feng S, Yu L, Tian F, Zhang H, et al. Protective effects of *Bacteroides fragilis* against lipopolysaccharide-induced systemic inflammation and their potential functional genes. Food Funct. 2022;13:1015–25. [PubMed: 35015021]
57. D'Amato A, Di Cesare Mannelli L, Lucarini E, Man AL, Le Gall G, Branca JJV, et al. Faecal microbiota transplant from aged donor mice affects spatial learning and memory via modulating hippocampal synaptic plasticity- and neurotransmission-related proteins in young recipients. Microbiome. 2020;8:140. [PubMed: 33004079]
58. Xu SS, Wang N, Huang L, Zhang XL, Feng ST, Liu SS, et al. Changes in the mucosa-associated microbiome and transcriptome across gut segments are associated with obesity in a metabolic syndrome porcine model. Microbiol Spectr. 2022;10:e0071722.
59. Liang JQ, Li T, Nakatsu G, Chen YX, Yau TO, Chu E, et al. A novel faecal Lachnoclostridium marker for the non-invasive diagnosis of colorectal adenoma and cancer. Gut. 2020;69:1248–57. [PubMed: 31776231]
60. Chen X, Levy JM, Hou A, Winters C, Azzam R, Sousa AA, et al. PSD-95 family MAGUKs are essential for anchoring AMPA and NMDA receptor complexes at the postsynaptic density. Proc Natl Acad Sci USA. 2015;112:E6983–6992. [PubMed: 26604311]
61. Ossenkoppele R, van der Kant R, Hansson O. Tau biomarkers in Alzheimer's disease: towards implementation in clinical practice and trials. Lancet Neurol. 2022;21:726–34. [PubMed: 35643092]
62. Scheltens P, De Strooper B, Kivipelto M, Holstege H, Chetelat G, Teunissen CE, et al. Alzheimer's disease. Lancet. 2021;397:1577–90. [PubMed: 33667416]
63. Lopez-Almela I, Romani-Perez M, Bullich-Vilarrubias C, Benitez-Paez A, Gomez Del EM, Frances R, et al. Bacteroides uniformis combined with fiber amplifies metabolic and immune benefits in obese mice. Gut Microbes. 2021;13:1–20.
64. Lee HB, Do MH, Jhun H, Ha SK, Song HS, Roh SW, et al. Amelioration of hepatic steatosis in mice through Bacteroides uniformis CBA7346-mediated regulation of high-fat diet-induced insulin resistance and lipogenesis. Nutrients. 2021;13:2989. [PubMed: 34578867]
65. Burrichter AG, Dorr S, Bergmann P, Haiss S, Keller A, Fournier C, et al. Bacterial microcompartments for isethionate desulfonation in the taurine-degrading human-gut bacterium *Bilophila wadsworthia*. BMC Microbiol. 2021;21:340. [PubMed: 34903181]
66. Gunalan A, Biswas R, Sridharan B, Elamurugan TP. Pathogenic potential of *Parabacteroides distasonis* revealed in a splenic abscess case: a truth unfolded. BMJ Case Rep. 2020;13:e236701.
67. De Vadder F, Kovatcheva-Datchary P, Goncalves D, Vinera J, Zitoun C, Duchampt A, et al. Microbiota-generated metabolites promote metabolic benefits via gut-brain neural circuits. Cell. 2014;156:84–96. [PubMed: 24412651]
68. Abdel-Haq R, Schlachetzki JCM, Glass CK, Mazmanian SK. Microbiome-microglia connections via the gut-brain axis. J Exp Med. 2019;216:41–59. [PubMed: 30385457]

69. Braniste V, Al-Asmakh M, Kowal C, Anuar F, Abbaspour A, Toth M, et al. The gut microbiota influences blood-brain barrier permeability in mice. Sci Transl Med. 2014;6:263ra158.
70. Wachsmuth HR, Weninger SN, Duca FA. Role of the gut-brain axis in energy and glucose metabolism. Exp Mol Med. 2022;54:377–92. [PubMed: 35474341]
71. Seo DO, O'Donnell D, Jain N, Ulrich JD, Herz J, Li Y, et al. ApoE isoform- and microbiota-dependent progression of neurodegeneration in a mouse model of tauopathy. Science. 2023;379:eadd1236.
72. Segain JP, Raingeard de la Bletiere D, Bourreille A, Leray V, Gervois N, Rosales C, et al. Butyrate inhibits inflammatory responses through NFkappaB inhibition: implications for Crohn's disease. Gut. 2000;47:397–403. [PubMed: 10940278]
73. Sun J, Wang F, Li H, Zhang H, Jin J, Chen W, et al. Neuroprotective effect of sodium butyrate against cerebral ischemia/reperfusion injury in mice. Biomed Res Int. 2015;2015:395895.
74. Luczynski P, McVey Neufeld KA, Oriach CS, Clarke G, Dinan TG, Cryan JF. Growing up in a bubble: using germ-free animals to assess the influence of the gut microbiota on brain and behavior. Int J Neuropsychopharmacol. 2016;19:pyw020.
75. Sarubbo F, Cavallucci V, Pani G. The Influence of Gut Microbiota on Neurogenesis: evidence and Hopes. Cells. 2022;11:382. [PubMed: 35159192]
76. Miko E, Csaszar A, Bodis J, Kovacs K. The maternal-fetal gut microbiota axis: physiological changes, dietary influence, and modulation possibilities. Life. 2022;12:424. [PubMed: 35330175]
77. Blanton LV, Charbonneau MR, Salih T, Barratt MJ, Venkatesh S, Ilkaveya O, et al. Gut bacteria that prevent growth impairments transmitted by microbiota from malnourished children. Science. 2016;351 10.1126/science.aad3311.
78. Maqsood R, Rodgers R, Rodriguez C, Handley SA, Ndao IM, Tarr PI, et al. Discordant transmission of bacteria and viruses from mothers to babies at birth. Microbiome. 2019;7:156. [PubMed: 31823811]
79. Ferretti P, Pasolli E, Tett A, Asnicar F, Gorfer V, Fedi S, et al. Mother-to-infant microbial transmission from different body sites shapes the developing infant gut microbiome. Cell Host Microbe. 2018;24:133–45.e135 [PubMed: 30001516]
80. Inczefi O, Bacquie V, Olier-Pierre M, Rincel M, Ringot-Destrez B, Ellero-Simatos S, et al. Targeted intestinal tight junction hyperpermeability alters the microbiome, behavior, and visceromotor responses. Cell Mol Gastroenterol Hepatol. 2020;10:206–8.e203 [PubMed: 32147490]
81. Abraham C, Abreu MT, Turner JR. Pattern recognition receptor signaling and cytokine networks in microbial defenses and regulation of intestinal barriers: implications for inflammatory bowel disease. Gastroenterology. 2022;162:1602–16.e1606 [PubMed: 35149024]
82. Browne HP, Neville BA, Forster SC, Lawley TD. Transmission of the gut microbiota: spreading of health. Nat Rev Microbiol. 2017;15:531–43. [PubMed: 28603278]
83. Brito IL, Gurry T, Zhao S, Huang K, Young SK, Shea TP, et al. Transmission of human-associated microbiota along family and social networks. Nat Microbiol. 2019;4:964–71. [PubMed: 30911128]
84. Fonareva I, Oken BS. Physiological and functional consequences of caregiving for relatives with dementia. Int Psychogeriatr. 2014;26:725–47. [PubMed: 24507463]
85. Valles-Colomer M, Blanco-Miguez A, Manghi P, Asnicar F, Dubois L, Golzato D, et al. The person-to-person transmission landscape of the gut and oral microbiomes. Nature. 2023;614:125–35. [PubMed: 36653448]
86. Thursby E, Juge N. Introduction to the human gut microbiota. Biochem J. 2017;474:1823–36. [PubMed: 28512250]
87. Eimer WA, Vassar R. Neuron loss in the 5XFAD mouse model of Alzheimer's disease correlates with intraneuronal Abeta42 accumulation and Caspase-3 activation. Mol Neurodegener. 2013;8:2. [PubMed: 23316765]
88. Dawson HN, Cantillana V, Jansen M, Wang H, Vitek MP, Wilcock DM, et al. Loss of tau elicits axonal degeneration in a mouse model of Alzheimer's disease. Neuroscience. 2010;169:516–31. [PubMed: 20434528]

89. Shen S, Lim G, You Z, Ding W, Huang P, Ran C, et al. Gut microbiota is critical for the induction of chemotherapy-induced pain. Nat Neurosci. 2017;20:1213–6. [PubMed: 28714953]

90. Kaliannan K, Wang B, Li XY, Kim KJ, Kang JX. A host-microbiome interaction mediates the opposing effects of omega-6 and omega-3 fatty acids on metabolic endotoxemia. Sci Rep. 2015;5:11276. [PubMed: 26062993]

91. Prizont R, Konigsberg N. Identification of bacterial glycosidases in rat cecal contents. Dig Dis Sci. 1981;26:773–7. [PubMed: 6793336]

92. Yang S, Gu C, Mandeville, Dong Y, Esposito E, Zhang Y, et al. Aneshethesia and surgery impair blood-brain barrier and cogntive function in mice. Front Immunol. 2017;8:902. [PubMed: 28848542]

93. Liufu N, Liu L, Shen S, Jiang Z, Dong Y, Wang Y, et al. Anesthesia and surgery induce age-dependent changes in behaviors and microbiota. Aging. 2020;12:1965–86. [PubMed: 31974315]

94. Zhao G, Nyman M, Jonsson JA. Rapid determination of short-chain fatty acids in colonic contents and faeces of humans and rats by acidified water-extraction and direct-injection gas chromatography. Biomed Chromatogr. 2006;20:674–82. [PubMed: 16206138]

95. Lai Z, Shan W, Li J, Min J, Zeng X, Zuo Z. Appropriate exercise level attenuates gut dysbiosis and valeric acid increase to improve neuroplasticity and cognitive function after surgery in mice. Mol Psychiatry. 2021;26:7167–87. [PubMed: 34663905]

96. Zhang Y, Xu Z, Wang H, Dong Y, Shi HN, Culley DJ, et al. Anesthetics isoflurane and desflurane differently affect mitochondrial function, learning, and memory. Ann Neurol. 2012;71:687–98. [PubMed: 22368036]

97. Aebersold R, Goodlett DR. Mass spectrometry in proteomics. Chem Rev. 2001;101:269–95. [PubMed: 11712248]

98. Li H, Jia J, Yang Z. Mini-Mental state examination in elderly chinese: a population-based normative study. J Alzheimers Dis. 2016;53:487–96. [PubMed: 27163822]

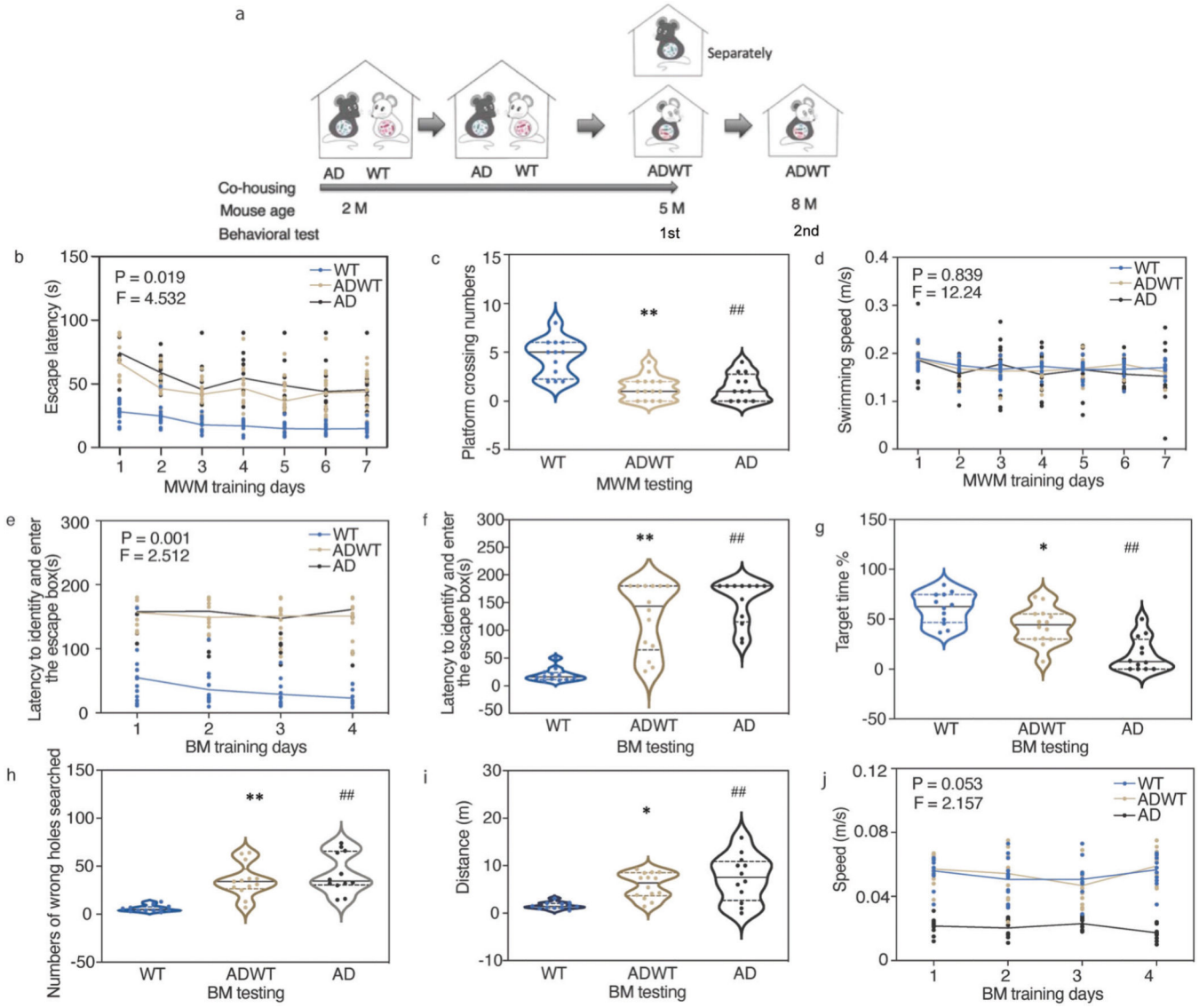

Fig. 1. WT mice developed cognitive impairment after co-housing with AD Tg mice.

a The 2-month-old WT mice co-housed with 2-month-old AD Tg mice for up to 3 months are defined as AD-exposed WT mice (ADWT mice). The ADWT mice were separated from AD Tg mice at age of 5-month-old. The behavioral tests of mice were performed at age of 5- and 8-month-old. After co-housing for 3 months, both AD Tg mice and ADWT mice developed cognitive impairment compared to the WT mice, as demonstrated by increased MWM escape latency during training days (**b**), decreased MWM platform crossing numbers on testing day (**c**), but no significant changes in swimming speed in MWM (**d**), increased latency to enter escape box during BM training days (**e**), and increased latency to enter escape box on BM testing day (**f**), decreased BM target time on testing day (**g**), increased number of wrong holes searched on BM testing day (**h**), and increased distance on testing day (**i**) compared to the WT mice. **j**. AD Tg, but not ADWT mice, had reduced speed compared to WT mice. Data are mean ± standard deviation or medians (with interquartile ranges), N = 12–14 mice in each experimental group. Two-way ANOVA with repeated

measurement and Bonferroni correction were used to analyze the data presented in **b**, **d**, **e**, and **j**. The *P* values refer to the interaction of group in MWM and BM training days. One-way ANOVA with Bonferroni correction were used to analyze the data presented in **c**, **f–i**. The *P* values refer to the differences of variables among the groups, $^{*}P < 0.05$; $^{\#\#}P < 0.01$. AD Alzheimer's disease, WT wild-type, ADWT AD-exposed WT, Tg transgenic, MWM Morris water maze, BM Barnes maze.

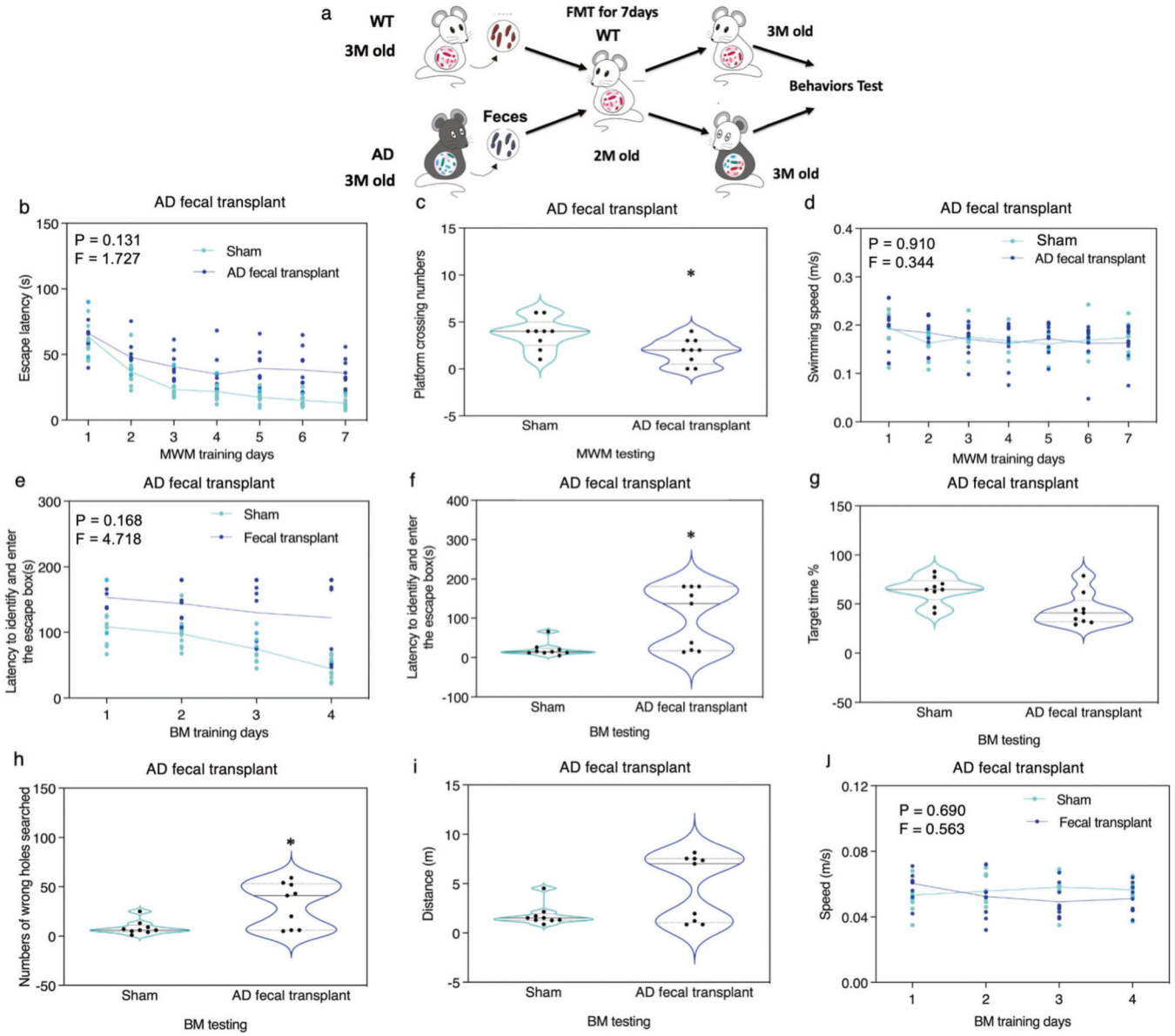

Fig. 2. WT mice developed cognitive impairment after fecal microbiota transplantation from AD Tg mice.

a The 2-month-old WT mice received gavage of fecal microbiota from the 3-month-old WT or AD Tg (5XFAD) mice for 7 days; the behaviors of the recipient WT mice were tested one month after the gavage at 3-month-old. The recipient WT mice received AD Tg mice fecal microbiota transplantation developed cognitive impairment compared to the WT mice received saline, demonstrated as slight trending of increased escape latency during training days (**b**), decreased platform crossing number on testing day (**c**), but no significant changes in swimming speed (**d**) of MWM. The recipient WT mice received fecal microbiota transplantation from AD Tg mice developed cognitive impairment compared to the WT mice received saline, demonstrated as slight trending of increased latency to enter escape box during BM training days (**e**), increased latency to enter escape box on BM testing day (**f**), but not significant changes in BM target time on testing day (**g**), increased number of

wrong holes searched on BM testing day (**h**), no significant changes on distance on BM testing day (**i**), and no significant changes on speed during training days (**j**). $N = 9$ mice in each experimental group. Two-way ANOVA with repeated measurement and Bonferroni correction was used to analyze the data presented in **b, d, e**, and **j**. The P values refer to the interaction of group in MWM and BM training days. Mann-Whitney U test was used to analyze the data presented in **c, f–i.** The P values refer to the differences of variables between the groups, $^{*}P < 0.05$. AD Alzheimer's disease, WT wild-type, Tg transgenic, MWM Morris water maze, BM Barnes maze, FMT fecal microbiota transplantation.

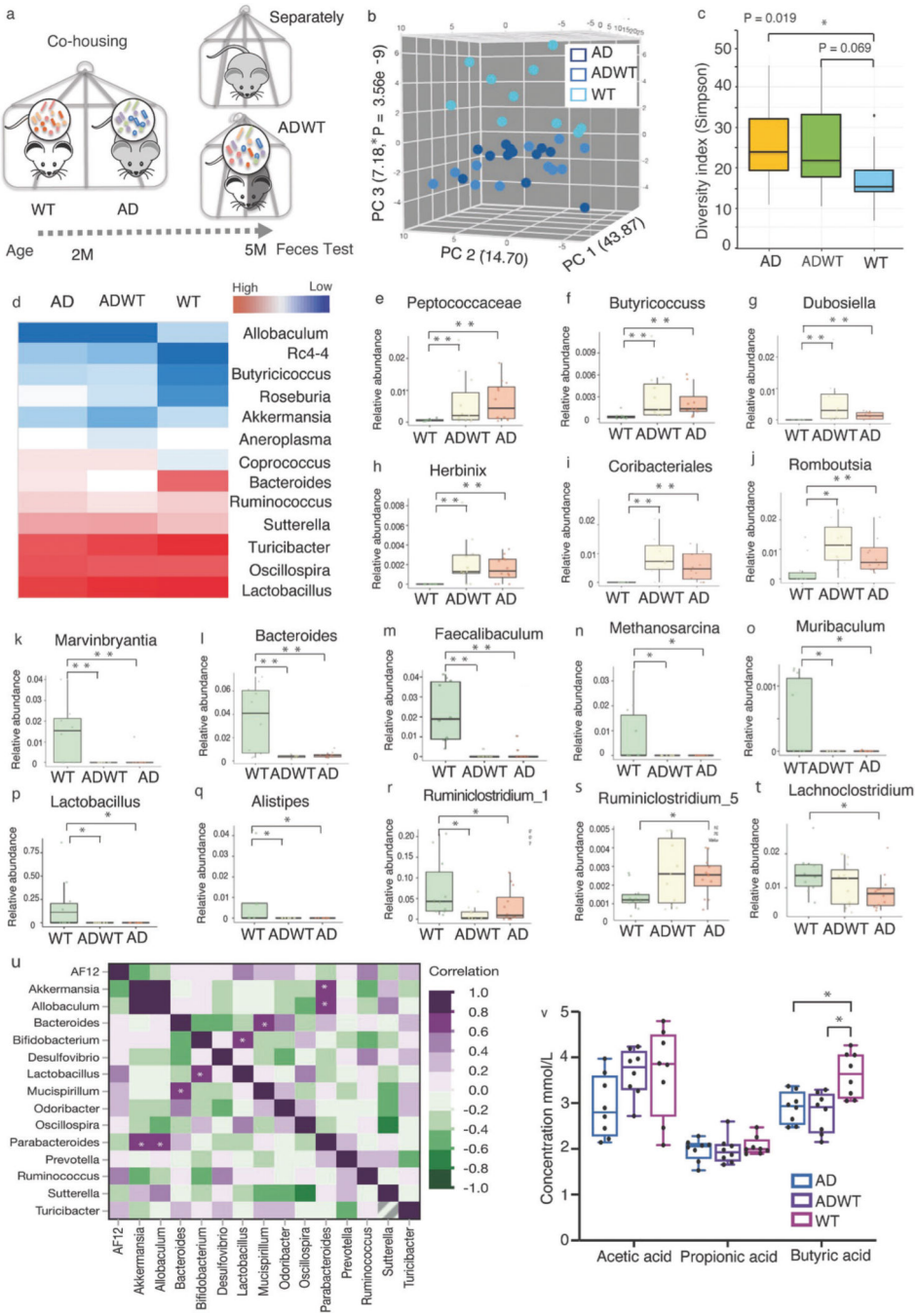

Fig. 3. ADWT mice acquired AD-associated gut microbiota dysbiosis after co-housing with AD Tg mice.

a Experimental design of fecal collection after 3 months co-housing. **b** Principal component analysis (PCA) using the Bray-Curtis dissimilarity metric among fecal samples of WT, ADWT, and AD Tg mice (P = 3.56e−9; permutational multivariate analysis of variance, PERMANOVA). Each dot represents an individual. PC1, PC2, and PC3 represent the percentage of variance explained by each coordinate. **c** Simpson diversity index was significantly higher in AD Tg mice and borderline significant higher in ADWT mice

compared to WT mice. **d** Heat map indicated the different changes in bacterial community structure represented as relative abundance shown in genus level analysis among the AD Tg, ADWT and WT mice. Relative to the WT mice, the AD Tg and ADWT mice had higher relative abundance of *Peptococcaceae* (**e**); *Butyricoccuss* (**f**); *Dubosiella* (**g**); *Herbinix* (**h**); *Coribacteriales* (**i**); *Romboutsia* (**j**), but lower relative abundance of *Marvinbryantia* (**k**); *Bacteroides* (**l**); *Faecalibaculum* (**m**); *Methanosarcina* (**n**); *Muribaculum* (**o**); *Lactobacillus* (**p**); *Alistipes* (**q**); *Ruminclostridium_1* (**r**). Relative to the WT mice, the AD Tg mice had higher relative abundance of *Ruminclostridium_5* (**s**) but lower relative abundance of *Lachnoclostridium* (**t**). **u** The heat map demonstrated the pair-wise correlative relationship between any pair of two bacteria among the WT, ADWT, and AD Tg mice. **v** Changes in fecal short-chain fat acids showed that the AD Tg and ADWT mice had less butyric acid amounts compared to the WT mice had. $N = 8–12$ biologically independent samples in each group. MaAsLin2 implementation were used for testing in microbiome profiles taxonomic result (**e–t**). One-way ANOVA with Bonferroni correction was used to analyze the data presented in (v). The P values refer to the differences of variables between the groups, $^{*}P < 0.05$; $^{**}P < 0.01$. AD Alzheimer's disease, WT wild-type, PC principal component, MaAsLin2, Microbiome Multivariable Association with Linear.

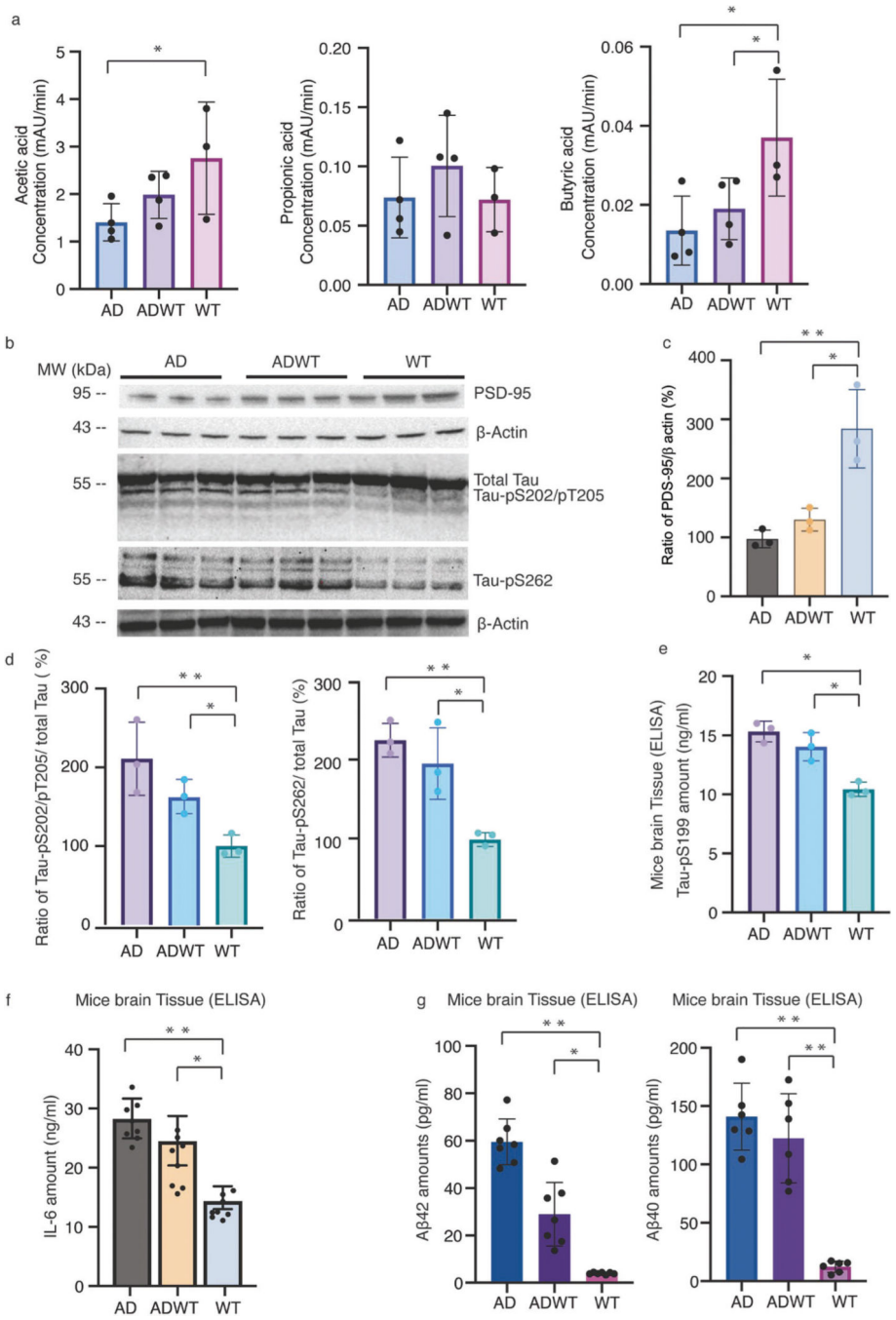

Fig. 4. Differences in brain levels of SCFAs, PSD-95, phosphorylated Tau, IL-6 and Aβ among AD Tg, ADWT and WT mice.

a The AD Tg mice had less brain acetic acid, but not propionic acid, levels compared to WT mice. Both the AD Tg and ADWT mice had less butyric acid levels in brain tissues compared to the WT mice. **b** Western blot showed that the AD Tg and ADWT mice had lesser amount of PSD-95, higher amounts of Tau-pS202/pT205 and Tau-pS262, but not total Tau, in the hippocampus compared to WT mice. **c** The quantification of the Western blots showed that the AD Tg and ADWT mice had a lesser ratio of PSD-95 to β-actin in the

hippocampus compared to the WT mice. **d** The quantification of the Western blots showed that the AD Tg and ADWT mice had a higher ratio of Tau-pS202/pT205 to total Tau and Tau-pS262 to total Tau in the hippocampus compared to the WT mice. **e** ELISA showed that AD Tg and ADWT mice had higher Tau-pS199 amounts in the hippocampus compared to WT mice. **f** The AD Tg and ADWT mice had higher amounts of IL-6 in the hippocampus compared to WT mice. **g** The AD Tg and ADWT mice had higher amounts of Aβ42 and Aβ40 in the hippocampus compared to the WT mice. $N = 3–8$ biologically independent samples in each group. One-way ANOVA with Bonferroni correction was used to analyze the data presented in **a, c–g** The P values refer to the differences of variables between the groups, $*P < 0.05$; $**P < 0.01$. AD Alzheimer's disease, WT wild-type, Tg transgenic, PSD-95 postsynaptic density 95, Interleukin 6 IL-6.

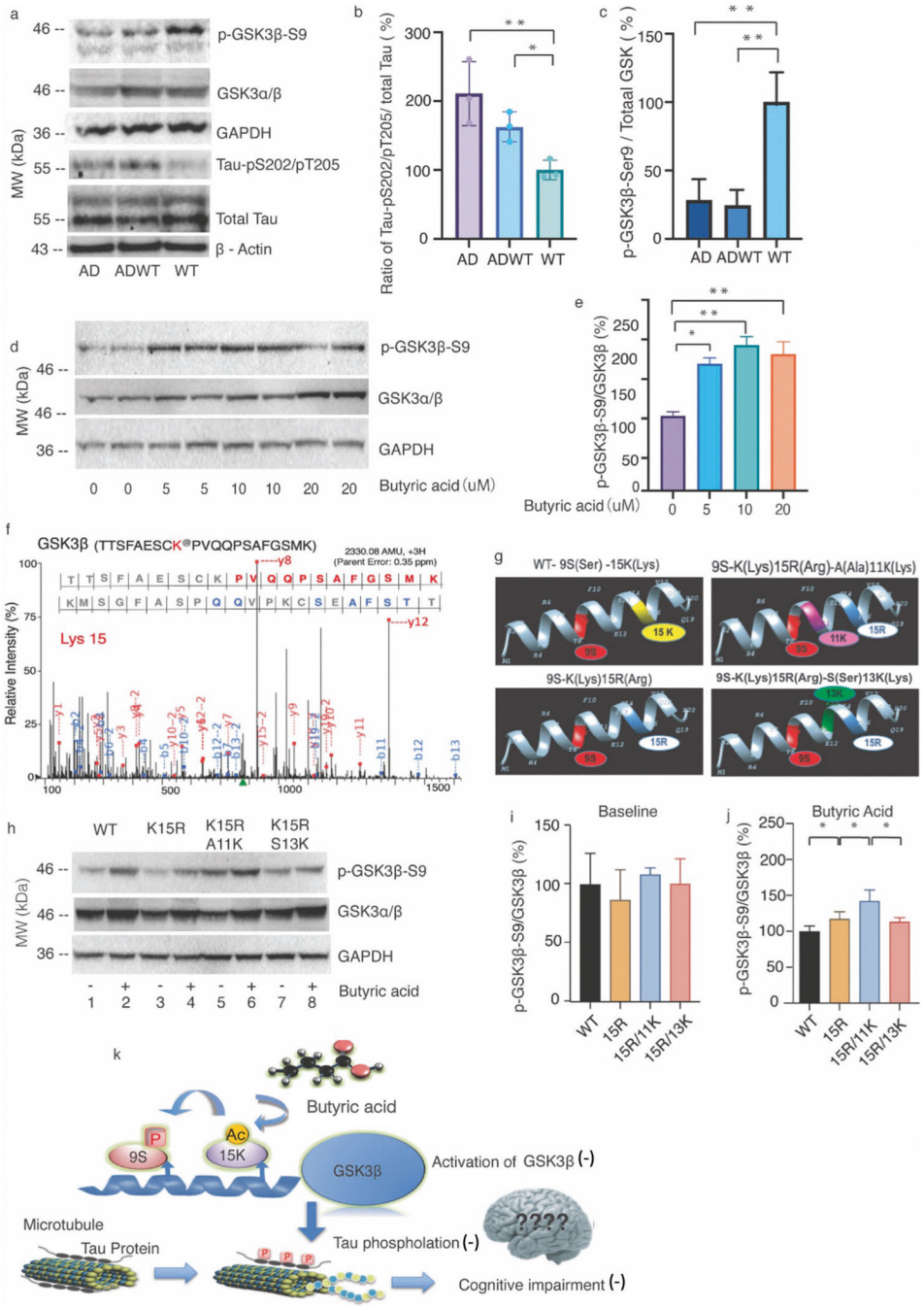

Fig. 5. Butyric acid increased p-GSK3β-S9 levels through lysine acetylation at position 15 of GSK3β.

a Western blot showed that the AD Tg and ADWT mice had higher amounts of Tau- pS202/pT205 and lower amounts of p-GSK3β-S9 in the hippocampus compared to WT mice. **b** The quantification of the Western blot demonstrated that AD Tg and ADWT mice had higher ratio of Tau-pS202/pT205 to total Tau in the hippocampus compared to WT mice. **c** The quantification of the Western blot demonstrated AD Tg and ADWT mice had lower ratio of p-GSK3β-S9 to total GSK3β in the hippocampus compared to WT mice. **d** Western

blot showed that the butyric acid increased p-GSK3β-S9 levels in HEK 293 T cells. **e** The quantification of the Western blot demonstrated the effects of butyric acid on increasing the ratios of p-GSK3β-S9 to GSK3β in HEK 293T cells. **f** Annotation of representative tandem mass spectra of Trypsin-GluC digested GSK3β, depicting K15 acetylation following the treatment of butyric acid in HEK 293T cells. **g** The computer-generated WT and three independent site-directed mutations (K15R, K15R/A11K, and K15R/S13K). **h** The effects of butyric acid on amounts of p-GSK3β-S9 and GSK3β in WT and the three independent site-directed mutants (K15R, K15R/A11K, and K15R/S13K) in HEK 293T cells. **i** The three mutations did not significantly change the baseline ratio of p-GSK3β-S9 to GSK3β. **j** However, the mutation of K15R increased the ratio of p-GSK3β-S9 to GSK3β, the mutation of K15R plus A11K had greater increases in the ratios of p-GSK3β-S9 to GSK3β than the mutations of K15R alone following the butyric acid treatment. Mutation of K15R/S13K had less effect on GSK3β phosphorylation at serine 9 than K15R/A11K following butyric acid treatment. **k** The hypothesized pathway showing that lysine at 15 of GSK3β may play an important role in the butyric acid-mediated inhibition of GSK3β activity, Tau phosphorylation and cognitive impairment. One-way ANOVA with Bonferroni correction was used to analyze the data presented in **b, c, e, i**, and **j**. The *P* values refer to the differences of variables between the groups, $*P < 0.05$; $**P < 0.01$. $N = 3$ biologically independent samples in each group. AD Alzheimer's disease, WT wild-type, p phosphorylated, pS phosphorylated serine, pT phosphorylated threonine, K lysine, R arginine, S serine, A alanine.

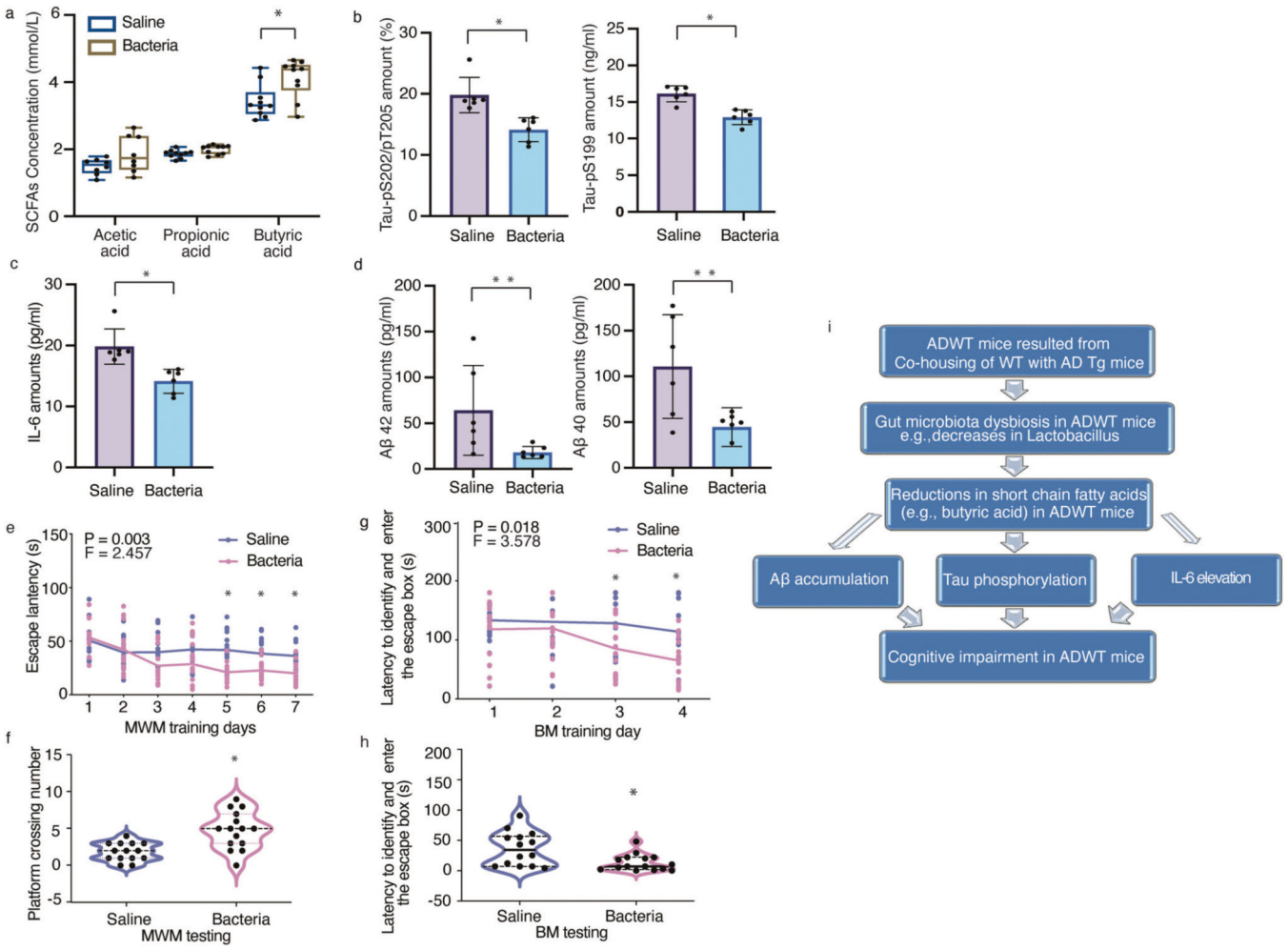

Fig. 6. Treatment with bacteria (*Lactobacillus* and *Bifidobacterium*) mitigated the behavioral and cellular changes in ADWT mice.

a The gavage of *Lactobacillus* plus *Bifidobacterium* (in the first 10 days in each month of the total 3 months) increased fecal butyric acid amounts of the ADWT mice compared to saline treatment. The gavage of *Lactobacillus* plus *Bifidobacterium* reduced the amounts of Tau-pS202/pT205 and Tau-pS199 (**b**), IL-6 (**c**) and Aβ42 and Aβ40 (**d**) in the hippocampus of the ADWT mice compared to saline treatment. Finally, the ADWT mice with gavage of *Lactobacillus* plus *Bifidobacterium* had better cognitive function compared to the ADWT mice with saline treatment, as demonstrated in MWM training (**e**), MWM testing (**f**), BM training (**g**), and BM testing (**h**). **i** The hypothesized pathway showing that ADWT mice, resulting from the co-housing of AD Tg and WT mice, acquire the AD-associated gut microbiota dysbiosis and reduced butyric acid amounts in gut and brain, which might cause Tau phosphorylation, IL-6 elevation and Aβ accumulation, leading to the cognitive impairment in the ADWT mice. Data are mean ± standard deviation or median (with interquartile range), $N = 6–15$ biologically independent samples in each group. Student's *t*-tests were used to analyze the data in **a–d**. Two-way ANOVA with repeated measurement and Bonferroni correction was used to analyze the data presented in **e** and **g**. Mann–Whitney *U* test was used to analyze the data in **f** and **h**. The *P* values refer to the differences of

variables or interaction between the groups, *$P < 0.05$; **$P < 0.01$. AD Alzheimer's disease, WT wild-type, p phosphorylated, pS phosphorylated serine, pT phosphorylated threonine, Interleukin 6 IL-6, MWM Morris water maze, BM Barnes maze.

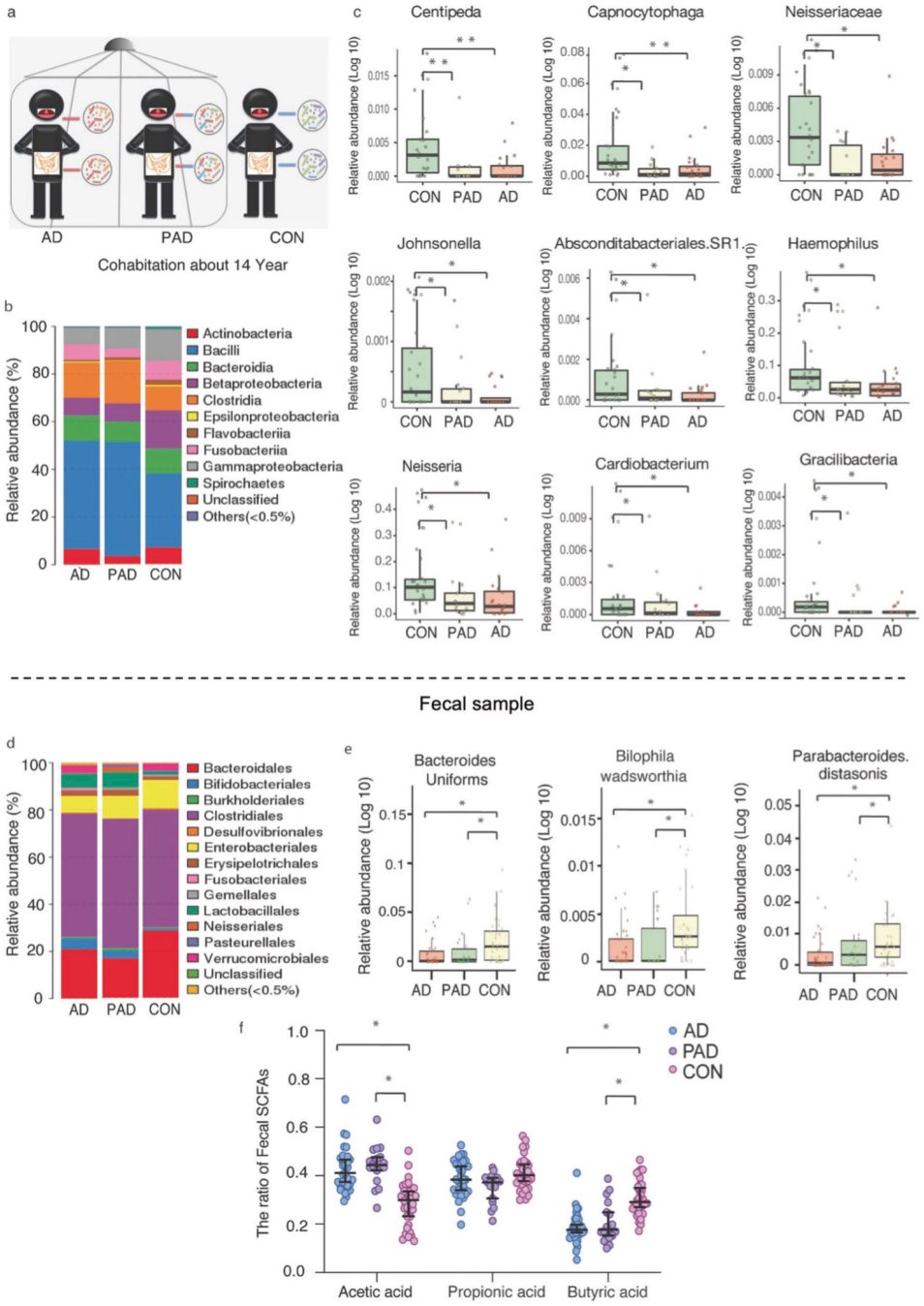

Fig. 7. Microbiota in oral and fecal samples of Alzheimer's disease (AD) patients, partners of AD patients (PAD), and control (CON) individuals.

a Schema of oral and fecal sample collection from AD, PAD, and CON. **b** The average taxonomic distribution of bacteria from oral 16 S RNA sequencing at the order level among the AD, PAD, and CON. **c** Relative abundances of *9 bacteria* in oral samples from AD and those from PAD were similar and significantly lower than those in CON. **d** The average taxonomic distribution of bacteria from fecal 16S RNA sequencing at the order level among the AD, PAD, and CON. **e** Relative abundances of 3 bacteria in fecal samples from AD and

PAD were similar and significantly lower than those in CON. **f** The ratios of acetic acid and butyric acid to total SCFAs in fecal samples among the three cohorts showed that the AD and PAD had higher acetic acid, but lower butyric acid compared to CON. There were the following biologically independent samples in each group of oral samples: AD (N = 19), PAD (N = 11), CON (N = 24) and fecal samples: AD (N = 39), PAD (N = 22), CON (N = 33). Microbiome Multivariable Association with Linear (MaAsLin2) implementation was used for testing in microbiome profiles taxonomic result (**c, e**). One-way ANOVA with Bonferroni correction was used to analyze the data in (**f**). The P values refer to the differences of variables between the groups, *P < 0.05; **P < 0.01. AD Alzheimer's disease, PAD partners of AD, CON control.

Key Resource table

Antigen	Host	Source	Catalog Clone	RRID	Concentration
Claudin-2	Rabbit	Turner Lab	Rb188–1	AB_2916077	1 μg/ml
Claudin-4	Rabbit	Abcam	ab210796	AB_2732879	0.1 μg/ml
E-cadherin	Mouse	Abcam	MAB1388	AB_1671631	1 μg/ml
Occludin	Rat	Cell Signaling	68534 clone 6B8A3	AB_2819194	1 μg/ml
ZO-1	Rat	Cell Signaling	R40.76	AB_628459	0.5 mg/ml
AF488-anti Mouse IgG F(ab′)2	Donkey	Jackson ImmunoResearch	715–546-151	AB_2340850	1 mg/ml
AF594-anti Rabbit IgG F(ab′)2	Donkey	Jackson ImmunoResearch	711–586-152	AB_2340622	1 mg/ml
AF647-anti Rat IgG F(ab′)2	Donkey	Jackson ImmunoResearch	712–606-153	AB_2340696	1 mg/ml
Tau-pS202/T205	Rabbit	ThermoFisher Scientific	MN1020B	AB_223648	0.1 mg/ml
Tau-pT181	Rabbit	ThermoFisher Scientific	701530	AB_2532491	0.5 mg/ml
Tau-pT217	Rabbit	ThermoFisher Scientific	44744	AB_2533741	n/a
Tau	Mouse	ThermoFisher Scientific	AHB0042	AB_2536235	0.5 mg/ml
GSK 3α/β	Rabbit	Cell Signaling	5676	AB_10547140	n/a
GSK3β-S9	Rabbit	Cell Signaling	9336	AB_331405	n/a
GAPDH	Rabbit	Cell Signaling	5174	AB_10622025	n/a
PSD95	Rabbit	Cell Signaling	2507	AB_2868428	n/a